Monte Carlo Ray Tracing for Coral Reef Light Calculations

Curtis D. Mobley

Sequoia Scientific, Inc.
2700 Richards Road, Suite 107
Bellevue, WA 98005

June 2018

Abstract

This note documents Monte Carlo ray tracing calculations used for the simulation of irradiances incident onto coral reef walls, slopes, and tops. The calculations described here are embedded into Curtis Mobley's generic backward Monte Carlo three-dimensional ray tracing code (named BMC3D). Previous versions of the BMC3D code have been used in Mobley and Sundman (2003), Lesser et al. (2018), and in studies of the 3D light field below ship hulls. The code developed here for coral reef simulations is denoted as BMC3D version 3.2, or BMC3D_coral. The ray tracing parts of the BMC3D_coral Fortran source code are documented with reference to this note.

One run of the code gives an estimate of one radiometric variable for a given reef geometry and reflectance properties; sensor location, type, and orientation; water IOPs at one wavelength, sea state (wind speed), and one or more sets of sun and atmospheric conditions. The choice of sensor type defines the radiometric variable, e.g., radiance, plane irradiance, or hemispherical scalar irradiance. These calculations use standard techniques of backward Monte Carlo simulation as developed by Gordon (1985) and others, and as described in *Light and Water* §6.2.

During ray tracing, whenever a ray leaves the sea surface, the current weight of the ray (relative to its initial weight of 1) is added to an accumulating weight for the sky angular bin containing the final ray direction after transmission through the wavy sea surface. Almost all of the BMC3D computer time is used for ray tracing within the water. These in-water calculations depend on the reef geometry and reflectance, water IOPs, and surface wind speed, but they do not depend on the sky conditions. Therefore, after the ray tracing is completed, the same accumulated weights in the sky angular bins can be used to compute the radiometric variable for a range of sun locations or atmospheric conditions. The final output of a run is then a table of the radiometric variable for sun zenith angles of 0, 10, 20,...,80 degrees, and sun azimuth angles from 0 (sun in front of the reef wall), to 90 deg (sun at right angles to the reef wall), to 180 deg (sun behind the reef wall) by steps of 15 deg. Thus one run of the code gives answers for one set of in-water parameters and one reef geometry, and many sets of sky parameters. The main code loops over wavelength so that the final output is an estimate of PAR for the chosen radiometric variable.

Selected results showing validation of the BMC3D_coral code are presented. Three appendices give the details of the ray tracing calculations for in-water scattering, ray initialization, and ray-sea surface interactions.

Contents

List of Figures

1 Reef Geometry

In this document, bold face denotes vectors or points in Euclidean 3-space, e.g., $\hat{\mathbf{x}}$ or $\mathbf{p}$. Figure 1 shows the reef geometry. The $(\hat{\mathbf{x}}, \hat{\mathbf{y}}, \hat{\mathbf{z}})$ directions define an "ocean" coordinate system that is convenient for specification of the reef top, reef slope, reef wall, and mean sea surface. This is a right-handed coordinate system with depth positive downward from 0 at the mean sea surface. This coordinate system is used for ray tracing. The reef wall faces the $+\hat{\mathbf{x}}$ direction. ($+\hat{\mathbf{x}}$ is also the downwind direction for the treatment of the wind-blown surface; see Appendix C.) The mean sea surface and the reef top, slope, and wall are defined by the (x, y, z) coordinates as follows:

Mean sea surface: the plane at $z = 0$

Reef top: the half plane defined by $x \leq x_{\mathrm{T}_1}, -\infty < y < \infty, z = z_{\mathrm{T}_1}$

Reef wall: the half plane defined by $x = x_{\mathrm{T}_2}, -\infty < y < \infty, z \geq z_{\mathrm{T}_2}$

Reef slope: the planar region defined by $x_{\mathrm{T}_1} < x < x_{\mathrm{T}_2}, -\infty < y < \infty, z_{\mathrm{T}_1} < z < z_{\mathrm{T}_2}$

Without loss of generality, the coordinate system can be centered above the reef wall, so that $x_{\mathrm{T}_2} = 0$.

The sun's azimuthal direction ϕ_{sun} is defined relative to the $+\hat{x}$ direction. When $\phi_{\mathrm{sun}} < 90$ deg, the reef wall is in the sun; when $\phi_{\mathrm{sun}} > 90$ deg, the reef wall is in the shade. The reef slope may be in the sun or the shade, depending on the sun's zenith angle θ_{sun}, azimuthal angle ϕ_{sun}, and the angle ψ of the slope surface. The reef top is always in the sun.

The numerical values for the reef top, slope, and wall boundaries; the reflectances of the reef top (R_{top}), slope (R_{slope}), and wall (R_{wall}); sun geometry; sensor depth, type, and orientation; water IOPs, etc., are specified at run time via a simple question-and-answer front end to the BMC3D code.

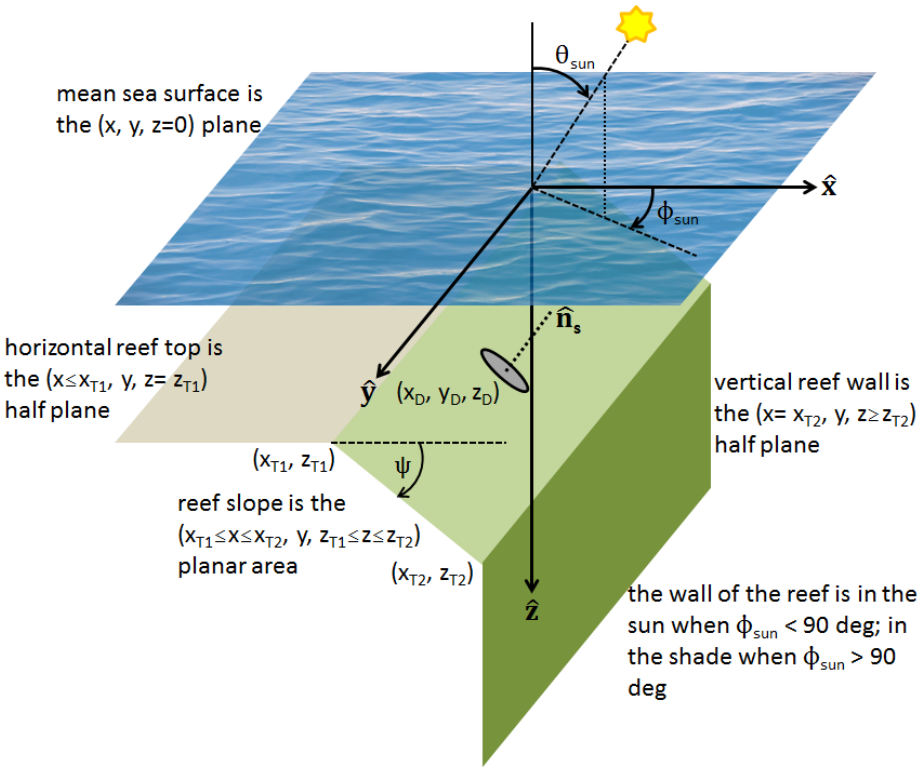

Figure 1: Geometry of the coral reef and the $(\hat{\mathbf{x}}, \hat{\mathbf{y}}, \hat{\mathbf{z}})$ ocean coordinate system used for ray tracing. The oval at (x_D, y_D, z_D) represents a detector placed at that location on the surface of the reef slope, whose normal is $\hat{\mathbf{n}}_S$.

2 Ray Tracing

There are innumerable options for light ray paths and interactions with the water body; reef wall, slope, and top; sea surface; and ocean bottom. Ray tracing in this geometry boils down to repeatedly finding the intersections of lines (the rays) and planes (the three reef surfaces and sea surface). The needed geometric entities are now defined in detail.

A *line* $\mathbf{L}$ refers to the infinite set of co-linear points defined by two points $\mathbf{r}_1 = [x_1, y_1, z_1]^{\mathrm{T}}$ and $\mathbf{r}_2 = [x_2, y_2, z_2]^{\mathrm{T}}$ in 3D space. (A superscript T, as here, denotes transpose, which in the present case gives column vectors. A subscript T denotes points in the top of the reef.) A *ray* $\mathbf{R}$ is the directed line segment from point $\mathbf{r}_1$ to point $\mathbf{r}_2$; the initial point of the ray is $\mathbf{r}_1$ and the final point is $\mathbf{r}_2$. A ray represents a beam of light, which travels in a straight line between scattering or reflection events and which is attenuated by absorption as it passes through the water. A ray is created at $\mathbf{r}_1$ (by initialization, reflection by a surface, or scattering within the water) and travels to $\mathbf{r}_2$, where it can be scattered again, unless it intersects a surface along the way. Note that a line is infinitely long, whereas a ray has finite length.

Just as a ray is a subset of a line, the coral surfaces are subsets of planes. The reef top is a half plane that is part of the plane defined by $z = z_{\mathrm{T}_1}$. The ray wall is a half plane that is contained in the plane defined by $x = x_{\mathrm{T}_2}$. The coral slope is part of a plane that is sloping downward from the

$\hat{\mathbf{x}}$ direction by an angle

$$\psi = \tan^{-1}\left(\frac{z_{\mathrm{T}_2} - z_{\mathrm{T}_1}}{x_{\mathrm{T}_2} - x_{\mathrm{T}_1}}\right). \tag{1}$$

If $x_{\mathrm{T}_1} < x_{\mathrm{T}_2}$, $0 < \psi < 90$ deg and the reef slope is facing "upward" toward the air-water surface. If $x_{\mathrm{T}_1} > x_{\mathrm{T}_2}$, $90 < \psi < 180$ and the reef slope is facing "downward" into the ocean depths, i.e. the reef slope is an "overhang".

The mean sea surface is the entire plane at $z = 0$.

Every line will eventually intersect each of the four planes containing the sea surface and reef top, slope, and wall (except for the case of a line being exactly parallel to one of the four planes, which is always a special case in Monte Carlo simulations). Figures 2a-2c illustrate some of these possibilities. In Fig. 2a, a ray travels from point $\mathbf{r}_1$ to point $\mathbf{r}_2$ as shown by the solid red arrow. The line containing this ray (the dotted red line) intersects the planes (dashed lines) containing the reef slope at point S, the reef wall at point W, the reef top at point T, and the air-water surface at point A. Open circles indicate intersections with these planes; filled circles indicate intersections with a reef or sea surface. This ray does not intersect any of the reef surfaces or the sea surface. In Fig. 2b, a ray with the same length and direction as the ray in Fig. 2a, but with a different starting point $\mathbf{r}_1$, intersects both the reef wall and slope. In the absence of the reef, this ray would travel to point $\mathbf{r}_2$. However, the ray intersects the reef wall first, so that is the point where the ray will be reflected by the reef. (The ray intersects the upward facing reef slope from below the slope, i.e., from within the coral, which would also be eliminated from consideration on physical grounds.) Figure 2c shows a ray intersecting the reef slope.
The ray tracing calculations fundamentally reduce to

- Finding the intersections of the line containing a ray with each of the four planes;
- Determining if the associated ray intersects one or more of the surfaces contained within the four planes;
- If the ray intersects more than one surface, determining which surface it intersects first.

The next sections develop the mathematics needed for these calculations.

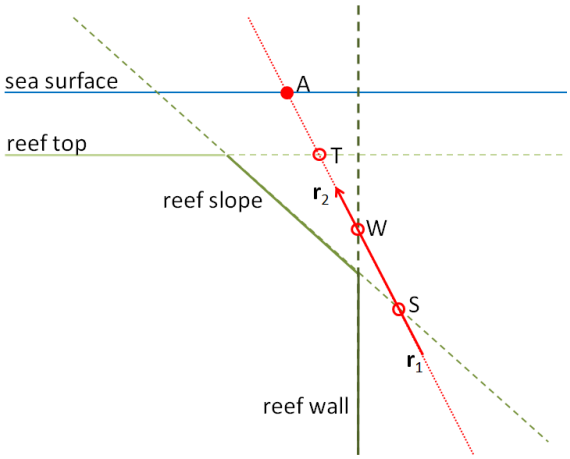

Figure 2a: Illustration of a ray that is within the water.

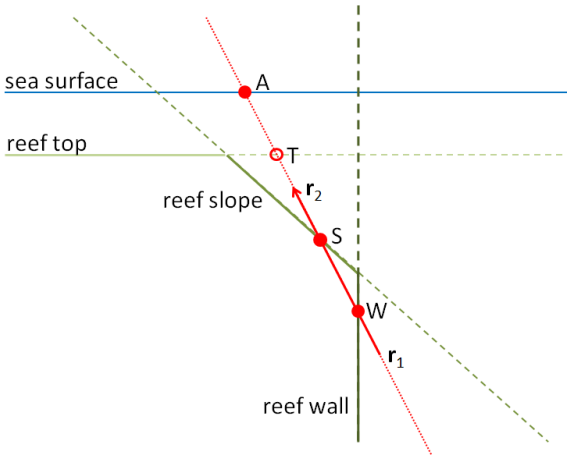

Figure 2b: Illustration of a ray that is incident onto the reef wall.

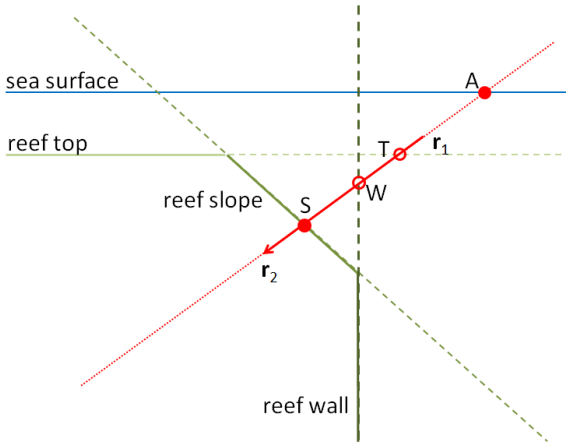

Figure 2c: Illustration of a ray that is incident onto the reef slope.

2.1 General Ray-Plane Intersections

A line $\mathbf{L}$ can be written in parametric form as

$$\mathbf{L} = \mathbf{r}_1 + (\mathbf{r}_2 - \mathbf{r}_1)t, \quad -\infty < t < \infty\,. \tag{2}$$

The corresponding ray $\mathbf{R}$ is then

$$\mathbf{R} = \mathbf{r}_1 + (\mathbf{r}_2 - \mathbf{r}_1)t, \quad 0 < t \leq 1\,. \tag{3}$$

A plane is determined by three non-colinear points $\mathbf{p}_1, \mathbf{p}_2, \mathbf{p}_3$; $\mathbf{p}_i = [p_{ix}, p_{iy}, p_{iz}]^T, i = 1, 2, 3$. A plane $\mathbf{P}$ can be written in parametric form as

$$\mathbf{P} = \mathbf{p}_1 + (\mathbf{p}_2 - \mathbf{p}_1)u + (\mathbf{p}_3 - \mathbf{p}_1)v, \quad -\infty < u, v < +\infty\,. \tag{4}$$

The intersection of a line and a plane can be found by setting the parametric forms for a line and a plane equal:

$$\mathbf{r}_1 + (\mathbf{r}_2 - \mathbf{r}_1)t = \mathbf{p}_1 + (\mathbf{p}_2 - \mathbf{p}_1)u + (\mathbf{p}_3 - \mathbf{p}_1)v\,.$$

This can be written in matrix form as

$$\begin{bmatrix} x_1 - p_{1x} \\ y_1 - p_{1y} \\ z_1 - p_{1z} \end{bmatrix} = \begin{bmatrix} x_1 - x_2 & p_{2x} - p_{1x} & p_{3x} - p_{1x} \\ y_1 - y_2 & p_{2y} - p_{1y} & p_{3y} - p_{1y} \\ z_1 - z_2 & p_{2z} - p_{1z} & p_{3z} - p_{1z} \end{bmatrix} \begin{bmatrix} t \\ u \\ v \end{bmatrix}\,. \tag{5}$$

After solving this equation for t, u, v, the value of t gives the distance from $\mathbf{r}_1$ at which the *line* intersects the plane. A negative value of t means that the plane lies "behind" the starting point of the ray, i.e., the plane is in the opposite direction of the ray as is the case for point A in Fig. 2c. If $0 \leq t \leq 1$, the associated *ray* also intersects the plane. If $t > 1$ or $t < 0$, the line intersects the plane, but the ray does not.

The point of intersection of the line with the plane is

$$\mathbf{L}_\mathrm{P} = \mathbf{r}_1 + (\mathbf{r}_2 - \mathbf{r}_1)t\,. \tag{6}$$

where the value of t is given by the solution of Eq. (5). The solution values of u, v, when substituted into Eq. (4), also give the point in the plane where the line intersects it.

We are free to choose points $\mathbf{p}_1, \mathbf{p}_2, \mathbf{p}_3$ as desired, so long as they lie in the plane and are not colinear. Therefore Eq. (5) can be tailored to the reef top, wall, and slope planes so as to simplify the matrix inversions required to obtain t, u, and v.

2.2 Ray-Reef Top Intersections

The plane containing the reef top can be defined by the three points

$$\mathbf{p}_1 = [0, 0, z_{T_1}]^\mathrm{T}\,, \tag{7a}$$
$$\mathbf{p}_2 = [0, 1, z_{T_1}]^\mathrm{T}\,, \tag{7b}$$
$$\mathbf{p}_3 = [1, 0, z_{T_1}]^\mathrm{T}\,. \tag{7c}$$

Equation (5) then simplifies to

$$\begin{bmatrix} x_1 \\ y_1 \\ z_1 - z_{\mathrm{T}_1} \end{bmatrix} = \begin{bmatrix} x_1 - x_2 & 0 & 1 \\ y_1 - y_2 & 1 & 0 \\ z_1 - z_2 & 0 & 0 \end{bmatrix} \begin{bmatrix} t_{\mathrm{T}} \\ u_{\mathrm{T}} \\ v_{\mathrm{T}} \end{bmatrix} ,$$

which has the solution

$$\begin{bmatrix} t_{\mathrm{T}} \\ u_{\mathrm{T}} \\ v_{\mathrm{T}} \end{bmatrix} = \frac{1}{z_1 - z_2} \begin{bmatrix} 0 & 0 & 1 \\ 0 & (z_1 - z_2) & -(y_1 - y_2) \\ (z_1 - z_2) & 0 & -(x_1 - x_2) \end{bmatrix} \begin{bmatrix} x_1 \\ y_1 \\ z_1 - z_{\mathrm{T}_1} \end{bmatrix} .$$

The value of t for the ray-reef top intersection is

$$t_{\mathrm{T}} = \frac{z_1 - z_{\mathrm{T}_1}}{z_1 - z_2} . \tag{8}$$

Recalling Eq. (6), the point $\mathbf{L}_{\mathrm{T}} = [x_{\mathrm{T}}, y_{\mathrm{T}}, z_{\mathrm{T}}]^{\mathrm{T}}$ where the line intersects the top plane is

$$x_{\mathrm{T}} = x_1 + (x_2 - x_1) \left(\frac{z_1 - z_{\mathrm{T}_1}}{z_1 - z_2} \right) , \tag{9a}$$

$$y_{\mathrm{T}} = y_1 + (y_2 - y_1) \left(\frac{z_1 - z_{\mathrm{T}_1}}{z_1 - z_2} \right) , \tag{9b}$$

$$z_{\mathrm{T}} = z_{\mathrm{T}_1} . \tag{9c}$$

Then if $x_{\mathrm{T}} \leq x_{\mathrm{T}_1}$, the ray intersects the reef top. It is easily verified that the same line-plane intersection point is obtained by insertion of the $u_{\mathrm{T}}, v_{\mathrm{T}}$ solution values into Eq. (4) along with the plane-defining points of Eq. (7).

(If the ray has $z_1 = z_2$, the ray is parallel to the top, or lies in the top, and there is no intersection for ray tracing. This can also be seen from the determinant of the matrix in Eq. (2.2), $D = -(z_1 - z_2)$, which is then zero, indicating that the equation has no solution. This rare event must be treated as a special case in the MC code.)

2.3 Ray-Reef Wall Intersections

With the coordinate system choice of $x_{\mathrm{T}_2} = 0$, the plane containing the reef wall can be defined by the three points

$$\begin{aligned} \mathbf{p}_1 &= [0, 0, 0]^{\mathrm{T}} , \\ \mathbf{p}_2 &= [0, 1, 0]^{\mathrm{T}} , \\ \mathbf{p}_3 &= [0, 0, 1]^{\mathrm{T}} . \end{aligned}$$

Equation (5) then simplifies to

$$\begin{bmatrix} x_1 \\ y_1 \\ z_1 - z_{\mathrm{T}_2} \end{bmatrix} = \begin{bmatrix} x_1 - x_2 & 0 & 0 \\ y_1 - y_2 & 1 & 0 \\ z_1 - z_2 & 0 & 1 \end{bmatrix} \begin{bmatrix} t_{\mathrm{W}} \\ u_{\mathrm{W}} \\ v_{\mathrm{W}} \end{bmatrix} ,$$

which has the solution

$$\begin{bmatrix} t_{\rm W} \\ u_{\rm W} \\ v_{\rm W} \end{bmatrix} = \frac{1}{x_1 - x_2} \begin{bmatrix} 1 & 0 & 0 \\ -(y_1 - y_2) & (x_1 - x_2) & 0 \\ -(z_1 - z_2) & 0 & (x_1 - x_2) \end{bmatrix} \begin{bmatrix} x_1 \\ y_1 \\ z_1 \end{bmatrix} .$$

The value of t for the ray-reef wall intersection is

$$t_{\rm W} = \frac{x_1}{x_1 - x_2} . \tag{10}$$

(If the ray has $x_1 = x_2$, the ray is parallel to the reef wall, or lies in it, and there is no intersection for ray tracing. This must be treated as a special case in the MC code.)

Recalling Eq. (6), the point $\mathbf{L}_{\rm W}$ where the line intersects the reef wall is

$$x_{\rm W} = 0 , \tag{11a}$$

$$y_{\rm W} = y_1 + (y_2 - y_1) \left(\frac{x_1}{x_1 - x_2} \right) , \tag{11b}$$

$$z_{\rm W} = z_1 + (z_2 - z_1) \left(\frac{x_1}{x_1 - x_2} \right) . \tag{11c}$$

Then if $z_{\rm W} \geq z_{\rm T_2}$, the ray intersects the reef wall.

2.4 Ray-Reef Slope Intersections

The reef slope equations are a bit more complicated because the reef slope is not parallel to one of the ocean coordinate planes.

The plane containing the reef slope can be defined by the three points

$$\mathbf{p}_1 = [0, 0, z_{\rm T_2}]^{\rm T} , \tag{12a}$$

$$\mathbf{p}_2 = [x_{\rm T_1}, 0, z_{\rm T_1}]^{\rm T} , \tag{12b}$$

$$\mathbf{p}_3 = [0, 1, z_{\rm T_2}]^{\rm T} . \tag{12c}$$

Equation (5) then becomes

$$\begin{bmatrix} x_1 \\ y_1 \\ z_1 - z_{\rm T_2} \end{bmatrix} = \begin{bmatrix} x_1 - x_2 & x_{\rm T_1} & 0 \\ y_1 - y_2 & 0 & 1 \\ z_1 - z_2 & z_{\rm T_1} - z_{\rm T_2} & 0 \end{bmatrix} \begin{bmatrix} t_{\rm S} \\ u_{\rm S} \\ v_{\rm S} \end{bmatrix} , \tag{13}$$

This equation has the solution

$$\begin{bmatrix} t_{\rm S} \\ u_{\rm S} \\ v_{\rm S} \end{bmatrix} = \frac{1}{D} \begin{bmatrix} -(z_{\rm T_1} - z_{\rm T_2}) & 0 & x_{\rm T_1} \\ (z_1 - z_2) & 0 & -(x_1 - x_2) \\ (y_1 - y_2)(z_{\rm T_1} - z_{\rm T_2}) & x_{\rm T_1}(z_1 - z_2) - (x_1 - x_2)(z_{\rm T_1} - z_{\rm T_2}) & -x_{\rm T_1}(y_1 - y_2) \end{bmatrix} \begin{bmatrix} x_1 \\ y_1 \\ z_1 - z_{\rm T_2} \end{bmatrix} . \tag{14}$$

where D is the determinant of the matrix in Eq. (13):

$$D = x_{\rm T_1}(z_1 - z_2) - (x_1 - x_2)(z_{\rm T_1} - z_{\rm T_2}) . \tag{15}$$

The (t, u, v) solution for the reef slope is

$$t_{\mathrm{S}} = \frac{1}{D}\left[-x_1(z_{\mathrm{T}_1} - z_{\mathrm{T}_2}) + x_{\mathrm{T}_1}(z_1 - z_{\mathrm{T}_2})\right] , \tag{16}$$
$$u_{\mathrm{S}} = \frac{1}{D}\left[x_1(z_1 - z_2) - (x_1 - x_2)(z_1 - z_{\mathrm{T}_2})\right] ,$$
$$v_{\mathrm{S}} = \frac{1}{D}\left[[x_1(y_1 - y_2) - y_1(x_1 - x_2)](z_{\mathrm{T}_1} - z_{\mathrm{T}_2}) + x_{\mathrm{T}_1}[y_1(z_1 - z_2) - (y_1 - y_2)(z_1 - x_{\mathrm{T}_2})]\right] .$$

Equations (6), (15), and (16) then give the point $\mathbf{L}_{\mathrm{S}}$ where the line intersects the reef slope:

$$x_{\mathrm{S}} = x_1 + (x_2 - x_1)t_{\mathrm{S}} , \tag{17a}$$
$$y_{\mathrm{S}} = y_1 + (y_2 - y_1)t_{\mathrm{S}} , \tag{17b}$$
$$z_{\mathrm{S}} = z_1 + (z_2 - z_1)t_{\mathrm{S}} . \tag{17c}$$

Then if $x_{\mathrm{T}_1} \le x_{\mathrm{S}} \le 0.0$ and $z_{\mathrm{T}_1} \le z_{\mathrm{S}} \le z_{\mathrm{T}_2}$, the ray intersects the reef slope at some point between the right edge of the reef top and the top edge of the reef wall.

2.5 Ray-Sea Surface Intersections

The plane containing the mean sea surface can be defined by the three points

$$\mathbf{p}_1 = [0, 0, 0]^T , \tag{18a}$$
$$\mathbf{p}_2 = [0, 1, 0]^T , \tag{18b}$$
$$\mathbf{p}_3 = [1, 0, 0]^T . \tag{18c}$$

Equation (5) then simplifies to

$$\begin{bmatrix} x_1 \\ y_1 \\ z_1 \end{bmatrix} = \begin{bmatrix} x_1 - x_2 & 0 & 1 \\ y_1 - y_2 & 1 & 0 \\ z_1 - z_2 & 0 & 0 \end{bmatrix} \begin{bmatrix} t_{\mathrm{A}} \\ u_{\mathrm{A}} \\ v_{\mathrm{A}} \end{bmatrix} , \tag{19}$$

which has the solution

$$\begin{bmatrix} t_{\mathrm{A}} \\ u_{\mathrm{A}} \\ v_{\mathrm{A}} \end{bmatrix} = \frac{1}{z_1 - z_2} \begin{bmatrix} 0 & 0 & 1 \\ 0 & (z_1 - z_2) & -(y_1 - y_2) \\ (z_1 - z_2) & 0 & -(x_1 - x_2) \end{bmatrix} \begin{bmatrix} x_1 \\ y_1 \\ z_1 \end{bmatrix} .$$

The value of t for the ray intersection with the air-water surface is

$$t_{\mathrm{A}} = \frac{z_1}{z_1 - z_2} . \tag{20}$$

Recalling Eq. (6), the point $\mathbf{L}_{\mathrm{A}} = [x_{\mathrm{A}}, y_{\mathrm{A}}, z_{\mathrm{A}}]^{\mathrm{T}}$ where the line intersects the mean sea surface is

$$x_{\mathrm{A}} = x_1 + (x_2 - x_1)\left(\frac{z_1}{z_1 - z_2}\right) , \tag{21a}$$
$$y_{\mathrm{A}} = y_1 + (y_2 - y_1)\left(\frac{z_1}{z_1 - z_2}\right) , \tag{21b}$$
$$z_{\mathrm{A}} = 0 . \tag{21c}$$

2.6 Oriented Normal to a Surface

Referring to Fig. 1, the upward or outward normal to a slope with $\psi < 90$ deg has $\hat{\mathbf{n}} \cdot \hat{\mathbf{z}} < 0$. This is because $\hat{\mathbf{n}}$ points generally upward (toward the sky), whereas $\hat{\mathbf{z}}$ points downward into the ocean. The included angle $\theta(\hat{\mathbf{n}}, \hat{\mathbf{z}})$ between $\hat{\mathbf{n}}$ and $\hat{\mathbf{z}}$ is then greater than 90 deg, making the dot product of these unit vectors, $\cos\theta(\hat{\mathbf{n}}, \hat{\mathbf{z}})$, less than zero.

For the choice of slope-defining points in Eq. (12), the outward normal is given by

$$\begin{aligned} \hat{\mathbf{n}}_{\mathrm{S}} &= \frac{(\mathbf{p_1} - \mathbf{p_2}) \times (\mathbf{p_1} - \mathbf{p_3})}{|(\mathbf{p_1} - \mathbf{p_2}) \times (\mathbf{p_1} - \mathbf{p_3})|} \\ &= \frac{(z_{\mathrm{T}_2} - z_{\mathrm{T}_1})\hat{\mathbf{x}} + x_{\mathrm{T}_1}\hat{\mathbf{z}}}{\left[(z_{\mathrm{T}_2} - z_{\mathrm{T}_1})^2 + x_{\mathrm{T}_1}^2 +\right]^{1/2}} \,. \end{aligned} \tag{22}$$

If $x_{\mathrm{T}_1} < 0$ the slope faces upward as in Fig. 1, and $\hat{\mathbf{n}} \cdot \hat{\mathbf{z}} = x_{\mathrm{T}_1} < 0$. If $x_{\mathrm{T}_1} > 0$ the slope folds over to become an overhang, $\hat{\mathbf{n}}$ points downward into the ocean, and $\hat{\mathbf{n}} \cdot \hat{\mathbf{z}} > 0$. Note in addition that if $x_{\mathrm{T}_1} = 0$, so that the slope is a vertical plane, $\hat{\mathbf{n}}$ points in the $\hat{\mathbf{x}}$ direction, i.e. outward from the vertical surface, into the water. For an upward-facing horizonal slope, $z_{\mathrm{T}_2} = z_{\mathrm{T}_1}, x_{\mathrm{T}_1} < 0$, and $\hat{\mathbf{n}} = -\hat{\mathbf{z}}$, as expected.

If the ray has $\hat{\mathbf{n}}_{\mathrm{S}} \cdot \mathbf{R} = \mathbf{0}$, the ray is perpendicular to the normal, i.e. the ray is parallel to the slope or lies in the slope, and there is no intersection for ray tracing. As always, this must be treated as a special case in the MC code.

It is easy to determine if a point is left ($x < 0$) or right ($x > 0$) of the reef wall plane, or above ($z < z_{\mathrm{T}_1}$) or below ($z > z_{\mathrm{T}_1}$) the reef top plane. To determine if a point $\mathbf{p}$ is above (on the water side) or below (on the coral side) the slope plane, proceed as follows. Point $\mathbf{p}_1 = [0, 0, z_{\mathrm{T}_2}]^{\mathrm{T}}$ lies in the slope plane. Then compute $\hat{\mathbf{n}}_{\mathrm{S}} \cdot (\mathbf{p} - \mathbf{p}_1)$ and test as follows:

$$\hat{\mathbf{n}}_{\mathrm{S}} \cdot (\mathbf{p} - \mathbf{p}_1) \begin{cases} > 0 & \text{if } \mathbf{p} \text{ is above the slope plane}\,, \\ = 0 & \text{if } \mathbf{p} \text{ lies in the slope plane}\,, \\ < 0 & \text{if } \mathbf{p} \text{ is below the slope plane}\,. \end{cases} \tag{23}$$

These equations can be used to test whether a ray intersects a reef surface from the water side as for point S in Fig. 2c, or from the coral side as for point S in Fig. 2b.

3 Finding Ray-Surface Intersections

The above equations give the tools needed to determine if a ray intersects the sea surface or the surface of the coral at any of the coral top, slope, or wall boundaries.

In most studies of light incident onto coral reefs for photosynthesis, the BMC3D_coral simulations initialize (emit) rays from points on the coral surfaces, e.g., at a pre-chosen depth on the face of the coral wall. Those initial rays then propagate into the water body, where they are repeatedly scattered until they occasionally past through the sea surface to be tallied as a contribution to the light incident onto the reef at the original point of emission. Some of these rays are scattered back onto the coral, where they are reflected back into the water. Some rays are scattered into downward directions until they are eventually killed because they have essentially no chance of making it back to the sea surface to be tallied. In any case, most of the ray-tracing calculations are for rays that

are wholly within the water. It therefore makes computational sense first to check for the most likely ray geometries, namely the ray being within the water to the right of the reef wall or above the reef slope or top. If the ray does not meet any of those conditions, it can then be checked for intersections with the reef itself or with the sea surface. For a given ray, then logic then proceeds as follows:

Given a ray defined by the initial and final points $\mathbf{r}_1$ and $\mathbf{r}_2$:

1. If $x_1 \geq 0$, $x_2 > 0$, and $z_2 > 0$, the ray is within the water to the right of the reef wall plane.

2. If $0 < z_1 < z_{\mathrm{T}_1}$ and $0 < z_2 < z_{\mathrm{T}_1}$, the ray is within the layer of water between the depth of the reef top plane and the mean sea surface.

3. If $\hat{\mathbf{n}}_{\mathrm{S}} \cdot (\mathbf{r}_2 - \mathbf{p}_1) > 0$ and $z_2 > 0$, the ray is in the water above the plane of the reef slope.

(The initial ray point $\mathbf{r}_1$ is always within the water or on the surface of the reef.)

If any of these conditions holds, the code proceeds with the calculations for creating (by scattering) a new ray at the in-water point $\mathbf{r}_2$, and the ray-tracing process repeats. If the tests above all fail, the code proceeds to test for other possibilities such as the in-water ray illustrated in Fig. 2a, or the intersection of the ray with the sea surface or the coral reef as seen in Figs. 2b and 2c. In that case the logic is as follows:

1. Use Eqs. (8), (10), (16), and (20) to find the distances from the ray initial point $\mathbf{r}_1$ to the intersection of the line with the reef top, wall, slope, and sea surface: $t_{\mathrm{T}}, t_{\mathrm{W}}, t_{\mathrm{S}}$, and t_{A} respectively. These t distances can have any positive or negative value.

2. Order the values of $(t_{\mathrm{T}}, t_{\mathrm{W}}, t_{\mathrm{S}}, t_{\mathrm{A}})$ from smallest to largest.

3. Any t value that is negative or greater than one indicates that the ray does not intersect the surface. Those surfaces need no further consideration. Examples are t_{A} in Fig. 2c, which is negative because the line intersects the surface "behind" the ray, and t_{T} in Fig. 2a, which is greater than one because the ray does not reach the plane containing the top surface.

4. The smallest positive value of t that is less than 1 identifies the first plane that is intersected by the ray. In Fig. 2b, for example, the value of t_{W} is less than the value of t_{S}. The ray therefore intersects the wall plane first. Further checking of the intersection point shows that, for this example, $z_{\mathrm{W}} > z_{\mathrm{T}_2}$, so that the ray intersects the reef wall. The ray will then be reflected by the wall at point W.

5. It may be than none of the rays satisfy the conditions for intersection with the coral surface even though one or more of the t values is between 0 and 1. This is the case for the ray of Fig. 2a because point S is to the right of the reef slope and point W is above the reef wall. In this case, the ray lies within the water, even though it was missed by the initial "in-water" checks.

4 Reflections by Coral Surfaces

If a ray is found to intersect the coral top, wall, or slope, it is the reflected at the point of intersection. The coral surfaces are assumed to be Lambertian reflectors with irradiance reflectances R_{top}, R_{wall}, and R_{slope}, respectively. In general these reflectances depend on wavelength and are determined by the type of coral surface being modeled.

This section develops the transformations needed to describe these reflections, which create new rays from rays that are incident onto the coral surface.

4.1 Lambertian Surfaces

A Lambertian surface reflects an incident ray into polar and azimuthal angles according to (see Appendix B or `http://www.oceanopticsbook.info/view/monte_carlo_simulation/level_2/the_brdf_as_a_pdf`)

$$\theta_r = \cos^{-1}(\sqrt{\mathfrak{R}_1})\,, \tag{24}$$

$$\phi_r = 2\pi\mathfrak{R}_2\,. \tag{25}$$

Here $\mathfrak{R}_1$ and $\mathfrak{R}_2$ are independently drawn uniform [0,1] random numbers, denoted by $\mathfrak{R} \sim U[0,1]$. The polar angle θ_r is relative to the outward normal to the Lambertian surface at $\theta_r = 0$. The azimuthal angle ϕ_r is relative to an x axis chosen for convenience in the surface. The distance traveled by the reflected ray is given by (*Light and Water* Eq. 6.5b or `http://www.oceanopticsbook.info/view/monte_carlo_simulation/introduction`)

$$\rho_r = \frac{1}{c}\ln\mathfrak{R}_3\,, \tag{26}$$

where c is the beam attenuation coefficient of the water. This ρ_r is the distance the newly created reflected ray will travel through the water body, unless it intersects another surface. The weight of the reflected ray is

$$w_r = R\,w_i\,, \tag{27}$$

where w_i is the weight of the incident ray, and R is the irradiance reflectance of the surface.

To implement these equations, local (at the point of the ray-surface intersection) coordinate systems for the reef top, wall, and slope must be defined. These are not the same as the ocean system seen in Fig. 1. In particular, the reef surfaces have outward normals that are not the same as $\hat{\mathbf{z}}$. The red arrows in Fig. 3 show local coordinate systems for the reef top, slope, and wall. (A local system for the mean sea surface is the same as for the reef top and is not shown.) Each of these systems has the local $\hat{\mathbf{x}}_\ell, \ell = \text{T, S, W, A}$ axis parallel to the ocean $\hat{\mathbf{y}}$ "along-reef" axis. The local $\hat{\mathbf{z}}_\ell$ axis is always the outward normal to the coral surface. The other axes depend on the surface. Thus for the reef top, $\hat{\mathbf{y}}_\text{T}$ is parallel to the ocean $\hat{\mathbf{x}}$ axis, and $\hat{\mathbf{z}}_\text{T}$ is antiparallel to $\hat{\mathbf{z}}$. For the reef wall, $\hat{\mathbf{y}}_\text{W}$ is parallel to the ocean $\hat{\mathbf{z}}$, and $\hat{\mathbf{z}}_\text{W}$ is parallel to $\hat{\mathbf{x}}$. In all cases, the local $\hat{\mathbf{y}}_\ell$ is obtained from $\hat{\mathbf{y}}_\ell = \hat{\mathbf{z}}_\ell \times \hat{\mathbf{x}}_\ell$.

After the angles of reflection are determined in the local system by Eqs. (24) and (25), these directions must be translated into the ocean system for ray further tracing.

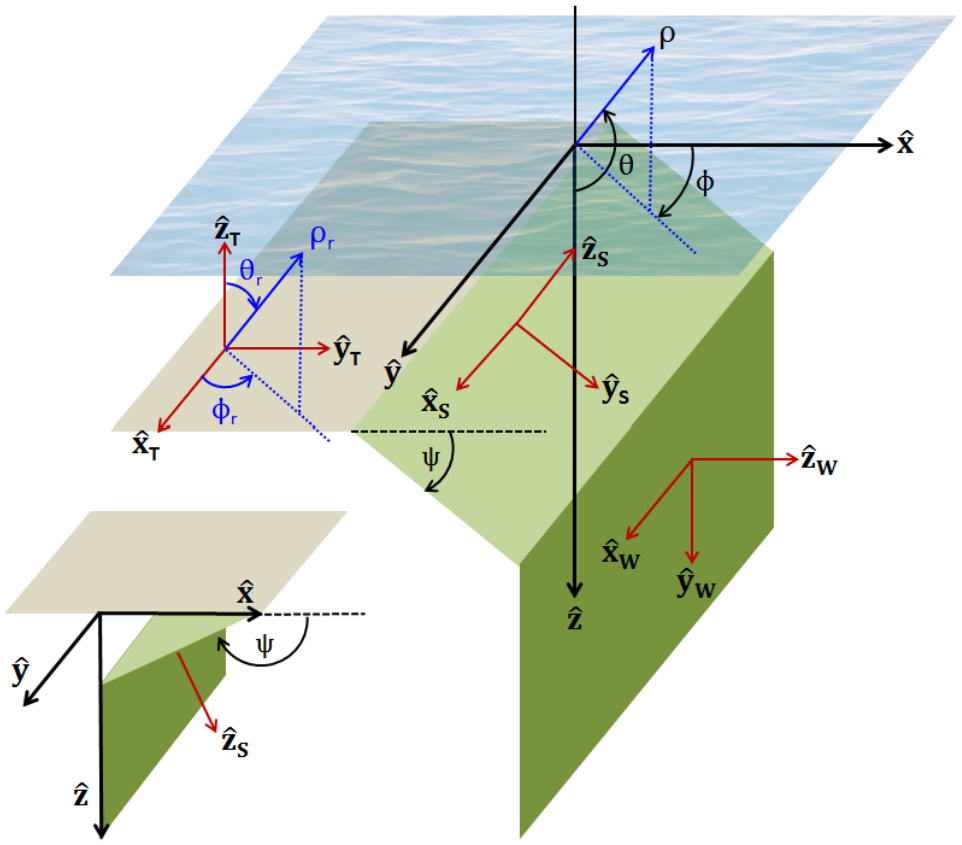

Figure 3: The red axes show the local coordinate systems for computation of reflected rays at the coral reef surfaces. The blue vector and $(\rho_r, \theta_r, \phi_r)$ coordinates in the reef top local system illustrate a reflected ray. The same vector translated to the origin of the ocean system shows the corresponding (ρ, θ, ϕ) coordinates in that system. The inset at the lower left illustrates an overhanging reef face, for which the reef slope ψ is greater than 90 deg and the outward normal to the reef is downward.

4.2 Local Coordinate System for the Reef Slope

The local system for the reef slope is the most general of these systems because its $\hat{\mathbf{y}}_S$ and $\hat{\mathbf{z}}_S$ axes are not parallel to any of the ocean system axes: $\hat{\mathbf{y}}_S$ is tilted downward from the ocean $\hat{\mathbf{x}}$ axis by an angle ψ as given by Eq. (1); $\hat{\mathbf{z}}_S$ is the same as the slope outward normal $\hat{\mathbf{n}}_S$ given by Eq. (22). The slope system is considered first; the other transformations can then be obtained by setting $\psi = 0$ to get the reef top transformation, and by setting $\psi = 90$ deg to get the reef wall transformation.

The transformation from the local slope system to the ocean system is obtained in two steps. Given a point (x_S, y_S, z_S), in the local system, first transform these coordinates into an intermediate (x', y', z') system obtained by a rotation about the local $\hat{\mathbf{x}}_S$ axis by an angle of ψ. (ψ as defined by Eq. (1) and shown in Fig. 3 corresponds to a rotation by $-\psi$ about the $\hat{\mathbf{x}}_S$ axis of that figure. Rotations by a positive angle $0 \le \psi \le 180$ deg are defined as counterclockwise when looking in the $-\hat{\mathbf{x}}_S$ direction.) This brings the $\hat{\mathbf{y}}_S$ axis parallel to the ocean $\hat{\mathbf{x}}$ axis, and brings the local $\hat{\mathbf{z}}_S$ into

the $-\hat{\mathbf{z}}$ direction. This transformation is given by

$$\begin{bmatrix} x' \\ y' \\ z' \end{bmatrix} = \begin{bmatrix} 1 & 0 & 0 \\ 0 & \cos\psi & \sin\psi \\ 0 & -\sin\psi & \cos\psi \end{bmatrix} \begin{bmatrix} x_{\mathrm{S}} \\ y_{\mathrm{S}} \\ z_{\mathrm{S}} \end{bmatrix} .$$

Now transform the intermediate values into the ocean coordinate system by interchanging the $\hat{\mathbf{x}}'$ and $\hat{\mathbf{y}}'$ axes, and by reversing the $\hat{\mathbf{z}}'$ axis:

$$\begin{bmatrix} x \\ y \\ z \end{bmatrix} = \begin{bmatrix} 0 & 1 & 0 \\ 1 & 0 & 0 \\ 0 & 0 & -1 \end{bmatrix} \begin{bmatrix} x' \\ y' \\ z' \end{bmatrix} .$$

Combining these two transformations then gives the transformation from local values of $(x_{\mathrm{S}}, y_{\mathrm{S}}, z_{\mathrm{S}})$ into ocean values (x, y, z):

$$\begin{bmatrix} x \\ y \\ z \end{bmatrix} = \begin{bmatrix} 0 & \cos\psi & \sin\psi \\ 1 & 0 & 0 \\ 0 & \sin\psi & -\cos\psi \end{bmatrix} \begin{bmatrix} x_{\mathrm{S}} \\ y_{\mathrm{S}} \\ z_{\mathrm{S}} \end{bmatrix} . \tag{28}$$

As seen in the previous section, the reflected ray is defined by values of the spherical coordinates $(\rho_r, \theta_r, \phi_r)$ obtained from Eqs. (26), (24), and (25), respectively. The cartesian coordinates of the reflected ray endpoint relative to the point where the previous ray intersected the surface are given in terms of spherical coordinates in the local system by

$$\begin{bmatrix} x_{\mathrm{S}} \\ y_{\mathrm{S}} \\ z_{\mathrm{S}} \end{bmatrix} = \begin{bmatrix} \rho_r \sin\theta_r \cos\phi_r \\ \rho_r \sin\theta_r \sin\phi_r \\ \rho_r \cos\theta_r \end{bmatrix} .$$

These values can be inserted into Eq. (28) to transform the spherical coordinates obtained from the Lambertian reflection calculations into cartesian values expressed in the ocean coordinate system used for ray tracing:

$$\begin{bmatrix} x \\ y \\ z \end{bmatrix} = \begin{bmatrix} 0 & \cos\psi & \sin\psi \\ 1 & 0 & 0 \\ 0 & \sin\psi & -\cos\psi \end{bmatrix} \begin{bmatrix} \rho_r \sin\theta_r \cos\phi_r \\ \rho_r \sin\theta_r \sin\phi_r \\ \rho_r \cos\theta_r \end{bmatrix} = \rho_r \begin{bmatrix} \cos\psi \sin\theta_r \sin\phi_r + \sin\psi \cos\theta_r \\ \sin\theta_r \cos\phi_r \\ \sin\psi \sin\theta_r \sin\phi_r - \cos\psi \cos\theta_r \end{bmatrix} . \tag{29}$$

This is the most general transformation needed for the current coral reef geometry.

The polar and azimuthal angles in the ocean system, (θ, ϕ), are given by

$$\cos\theta = \frac{z}{\rho} \tag{30}$$

$$\tan\phi = \frac{y}{x} . \tag{31}$$

Thus from Eq. (29)

$$\cos\theta = \frac{z}{\rho} = \sin\psi \sin\theta_r \sin\phi_r - \cos\psi \cos\theta_r \tag{32}$$

$$\tan\phi = \frac{y}{x} = \frac{\sin\theta_r \cos\phi_r}{\cos\psi \sin\theta_r \sin\phi_r + \sin\psi \cos\theta_r} . \tag{33}$$

The ray length is independent of coordinate system, so $\rho = \rho_r$.

In practice, these equations for (θ, ϕ) in the ocean coordinate system need not be evaluated because the reflected ray is defined in the ocean system by the cartesian coordinates $\mathbf{r}_1 = [x_{\rm S}, y_{\rm S}, z_{\rm S}]^{\rm T}$ and $\mathbf{r}_2 = [x, y, z]^{\rm T}$, where the ray end point values relative to the starting point come from Eq. (29). Thus the ray endpoint in the ocean system is given by

$$\mathbf{r}_2 = \begin{bmatrix} x_{\rm S} \\ y_{\rm S} \\ z_{\rm S} \end{bmatrix} + \begin{bmatrix} x \\ y \\ z \end{bmatrix} . \tag{34}$$

4.3 Reflection at the Reef Top

The local right-handed coordinate system $(x_{\rm T}, y_{\rm T}, z_{\rm T})$ used for reflection computations at the reef top is obtained by setting $\psi = 0$ in the slope equations of the previous section. The result is

$$\begin{bmatrix} x \\ y \\ z \end{bmatrix} = \rho_r \begin{bmatrix} \sin\theta_r \sin\phi_r \\ \sin\theta_r \cos\phi_r \\ -\cos\theta_r \end{bmatrix} . \tag{35}$$

For the reef-top local coordinate system $(x_{\rm T}, y_{\rm T}, z_{\rm T})$, it is easy seen by inspection of Fig. 3 that the ocean-system values (θ, ϕ) are related to the local values of (θ_r, ϕ_r) by

$$\theta = \pi - \theta_r \tag{36}$$

$$\phi = \phi_r - \frac{\pi}{2} . \tag{37}$$

Use of Eq. (35) in Eqs. (30) and (31), or setting $\psi = 0$ in Eqs. (32) and (33), gives the ocean-system (θ, ϕ) corresponding to the angles (θ_r, ϕ_r) in the reef-top local system,

$$\cos\theta = \frac{z}{\rho} = \frac{-\rho_r \cos\theta_r}{\rho_r} = -\cos\theta_r$$

$$\tan\phi = \frac{y}{x} = \frac{\rho_r \sin\theta_r \cos\phi_r}{\rho_r \sin\theta_r \sin\phi_r} = -\cot\phi_r .$$

These equations are satisfied by the relations seen in Eqs. (36) and (37), as previously noted.

4.4 Reflection at the Reef Wall

Point W in Fig. 2b illustrates a ray originally directed from point $\mathbf{r}_1$ to point $\mathbf{r}_2$, but which intersects the reef wall at point W. For the reef wall, the local coordinate system is given by setting $\psi = 90$ deg in Eq. (29):

$$\begin{bmatrix} x \\ y \\ z \end{bmatrix} = \begin{bmatrix} 0 & 0 & 1 \\ 1 & 0 & 0 \\ 0 & 1 & 0 \end{bmatrix} \begin{bmatrix} \rho_r \sin\theta_r \cos\phi_r \\ \rho_r \sin\theta_r \sin\phi_r \\ \rho_r \cos\theta_r \end{bmatrix} = \rho_r \begin{bmatrix} \cos\theta_r \\ \sin\theta_r \cos\phi_r \\ \sin\theta_r \sin\phi_r \end{bmatrix} . \tag{38}$$

The relations between (θ, ϕ) and the reef-wall (θ_r, ϕ_r) are then

$$\cos\theta = \sin\theta_r \sin\phi_r \tag{39}$$

$$\tan\phi = \tan\theta_r \cos\phi_r . \tag{40}$$

These equations for (θ, ϕ) are more complicated than Eqs. (36) and (37). In particular, each of θ and ϕ depends on both θ_r and ϕ_r.

4.5 Reflection and Transmission at the Sea Surface

If a ray crosses the mean sea surface at $z = 0$, it is processed using the Cox-Munk wind speed-wave slope statistics for a wind-blown sea surface, Snel's law of refractioin, and Fresnel's law of reflection for unpolarized light. In all cases there is a ray reflected back into the water. The weight of the reflected ray is determined from the angle of the incident ray onto the (generally) tilted water surface and Fresnel's law. There is usually a ray transmitted into the air, whose direction in the air is determined by Snel's law and whose weight is obtained from one minus the fraction of the reflected-ray weight. In some cases there may be total internal reflection, in which case the reflected ray has the same weight as the incident ray and there is no transmitted ray. The details of these calculations are given in Appendix C.

The weight of the transmitted ray is added to an accumulating weight sum for the sky $(\Delta\theta, \Delta\phi)$ bin in the direction of the transmitted ray. The default bin sizes are a 5 deg half-angle polar cap and 10×15 deg $\Delta\theta \times \Delta\phi$ bins except for the bins nearest the horizon, which are 15 deg in $\Delta\theta$.

Suppose a ray emitted by the source with weight $w = 1$ eventually (usually after many scatterings and reflections) reaches the sky in direction (θ, ϕ) with weight $0 < w \leq 1$. The principle of electromagnetic reciprocity (based on the time-invariance of Maxwell's equations), says that a ray traveling from the sky in direction $(180 - \theta, 180 + \phi)$ (the opposite direction of the ray reaching the sky) will retrace the original ray's path and reach the detector.

At the end of the ray tracing, a fraction f_{ij} of the total weight of the rays emitted by the detector reaches sky bin $(\Delta\theta_i, \Delta\phi_j)$. Thus by reciprocity a fraction f_{ij} of the sky radiance averaged over $(\Delta\theta_i, \Delta\phi_j)$ will reach the detector. This is the connection between the sky radiance distribution and the radiance received by the detector, which when integrated over the detector's angular response generates the irradiance received by the detector. The entire purpose of the ray tracing is to estimate the weight array f_{ij}. The f_{ij} values depend on the sensor type and orientation, water IOPs, reef geometry, and depth, but not on the sky conditions. Any sky radiance distribution can then be applied to the computed f_{ij} to obtain the at-sensor irradiance for the given sky radiance distribution. This is the essence of the backward Monte Carlo algorithm.

4.6 Use of the Preceding Equations

It may be worthwhile to summarize the use of the preceding equations as employed in the Monte Carlo code. The algorithm is as follows.

Initial Ray: An initial ray starting at point $\mathbf{r}_1 = [x_1, y_1, z_1]^{\mathrm{T}}$ is predicted to reach final point $\mathbf{r}_2 = [x_2, y_2, z_2]^{\mathrm{T}}$, with both points expressed in the ocean coordinate system. (See Appendix B for the details of how initial rays are created.)

Ray-Surface Intersection: Suppose it is found by the tests of §3 that this initial ray intersects one of the coral surfaces. The most general surface is that of the coral slope, which contains the coral top and wall as special cases of the slope angle ψ, so consider that case. The point

of intersection of the ray with the slope, $\mathbf{p}_S = [x_\mathrm{S}, y_\mathrm{S}, z_\mathrm{S}]^\mathrm{T}$, is given by Eqs. (15), (16), and (17). These coordinates are in the ocean system.

Ray Reflection: The ray is reflected into polar and azimuthal directions (θ_r, ϕ_r) according to Eqs. (24) and (25). These directions are relative to the local coordinate system at the point of intersection, as shown in Fig. 3. The reflected ray will travel a distance ρ_r given by Eq. (26); the weight of the reflected ray is given by Eq. (27).

New Ray Initial Point: The intersection point $\mathbf{p}_S$ becomes the initial point $\mathbf{r}_1 = [x_1, y_1, z_1]^\mathrm{T}$ for the reflected ray.

New Ray Final Point: Equation (29) is used to convert the local directions and ray length to the end point (x, y, z) of the reflected ray in the ocean coordinate system, relative to the initial point of the new ray. The end point of the new ray in the ocean system is then given by Eq. (34).

Recursion: The new ray from $\mathbf{r}_1$ to $\mathbf{r}_2$ is now traced just as was the initial ray.

In practice, the general Eq. (29) is replaced by its simpler forms (35) and (38) if the initial ray intersects the reef top or reef wall, respectively. This reduces the number of evaluations of trigonometric functions, which reduces the computational costs when tens or hundreds of millions of rays must be traced.

Note that it is not necessary explicitly to compute the reflected-ray directions (θ, ϕ) in the ocean system, as seen in Eqs. (32) and (33). Those equations are included above for completeness of the discussion and to facilitate checking the code, as discussed in the §5.1.

5 Code Validation

The version 1.0 Monte Carlo ray tracing code was developed in 1999 and has been used in several studies since then. That code has been well debugged and validated against HydroLight for 1D geometries for which both HydroLight and the BMC3D code are applicable. However, the new options for ray interactions with the coral reef required a lot of new code, which gives additional opportunities for errors.

5.1 Angle Distributions

A qualitative check on the fundamental reef-to-ocean coordinate transformation of Eq. (29) can be made via the statistical distributions of the reflectance angles as seen in Eqs. (32) and (33).

Panel (a) of Fig. 4 shows the statistical distributions of the Lambertian reflection angles (θ_r, ϕ_r) as generated by Eqs. (24) and (25), respectively, for sequences of 10^6 randomly generated sets of angles (each set of angles was generated with an independent set of random numbers). The resulting angles were collected into 2 deg bins for creation of the plotted histograms. The ϕ_r distribution is uniform over 0 to 360 deg in accordance with Eq. (25). The ϕ distribution is also 0 to 360, although the two-argument inverse tangent function $\tan^{-1}(y, x)$ returns values in the -180 to +180 deg range, which is equivalent and is what is plotted here. The range of values for θ_r is 0 to 90 deg, i.e. all "upward" directions in the reef-top coordinate system. However, the distribution of

θ_r is non-uniform, as expected from Eq. (24). It must be remembered that a Lambertian surface by definition reflects *radiance* equally into all *solid angles*, not equally into all θ directions. This means that *individual rays* must be reflected from each *point* on a Lambertian surface according to Eq. (24). See `http://www.oceanopticsbook.info/view/monte_carlo_simulation/level_2/the_brdf_as_a_pdf` for further discussion.

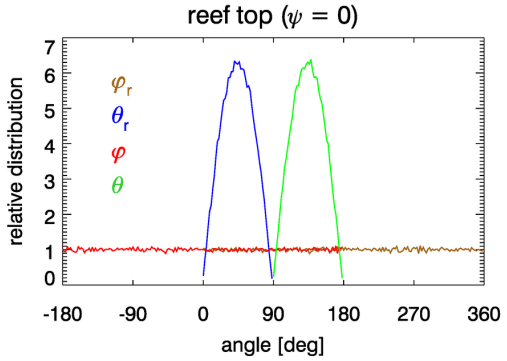

(a) Distributions reflection angles in the reef-top system and in the ocean systems.

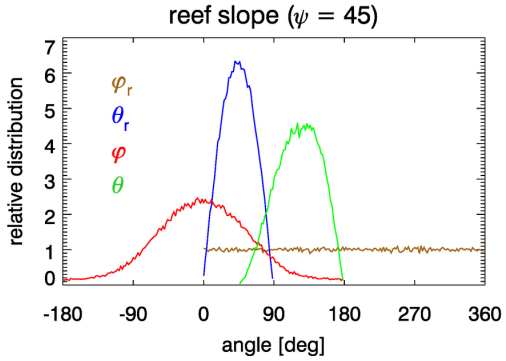

(b) Distributions reflection angles in the reef-slope system and ocean systems for $\psi = 45$ deg.

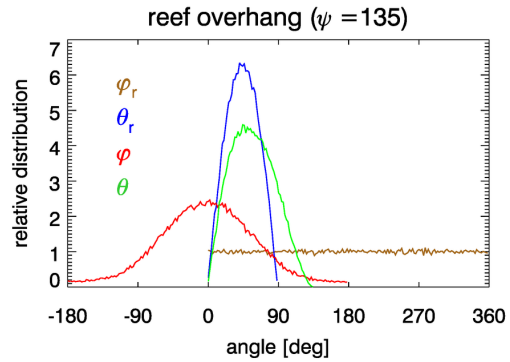

(c) Distributions reflection angles in the reef-slope system and ocean systems for $\psi = 135$ deg.

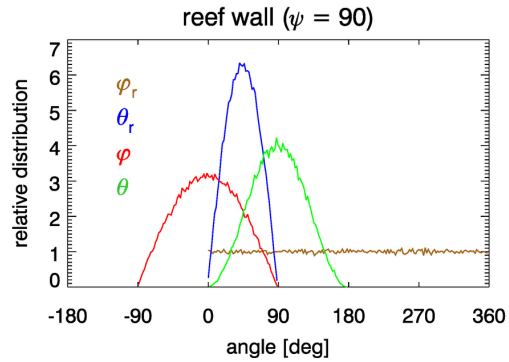

(d) Distributions of reflection angles in the reef-wall and ocean systems

Figure 4: Distributions of Lambertian reflection angles in the reef and ocean coordinate systems. The simulations were for 10^6 reflections and angle bin sizes of 2 deg.

Figure 4(b) shows the same simulation for the reef slope with $\psi = 45$ deg. The reflected angles were generated using the same sets of random numbers as for the reef top; the (θ_r, ϕ_r) values are therefore identical to those of panel (a). To understand the (θ, ϕ) distributions, keep the following in mind. A ray heading "straight down the slope" (in the $+\hat{\mathbf{y}}_S$ direction) has $(\theta = 45, \phi = 0)$. A ray traveling normal to the surface (parallel to $+\hat{\mathbf{z}}_S$) has $(\theta = 135, \phi = 0)$. A ray heading "straight up the slope" (in the $-\hat{\mathbf{y}}_S$ direction) has $(\theta = 135, \phi = 180)$. A ray traveling "straight up" (toward the sea surface, has $\theta = 180$. The end result is distributions of θ between 35 and 180 deg, and of ϕ between -180 and +180 deg (or equivalently 0 to 360 deg). Figure 4(c) shows that the distributions for a reef overhang with $\psi = 135$ deg are similar, except that the range of θ is 0 to 135 deg, for

rays heading from straight down to straight up the overhang.

Finally, Fig. 4(d) shows the same simulation for the reef wall. Now the range of θ values is 0 to 180 deg and the range of ϕ values is -90 to +90 deg in the ocean system. In the reef-wall local system the θ_r values are 0 to 90 for rays traveling away from the vertical reef surface, but those rays can be traveling "up" or "down" in the ocean system, i.e., anything from $\theta = 0$ for a ray heading straight down to $\theta = 180$ deg for a ray heading straight up (toward the sea surface). The ϕ values range from -90 deg for a ray heading in the $-\hat{\mathbf{y}}$ direction to +90 deg for rays heading in the $+\hat{\mathbf{y}}$ direction of the ocean system. These directions correspond to rays traveling toward the "right" (away from the reef wall) in the $+\hat{\mathbf{x}}$ half space in Fig. 3.

5.2 Ray Tracks

Another qualitative check on the code comes from visual inspection of plotted of ray tracks to see if the ray tracks behaved as expected. Figure 5 shows an example plot of this type. In this simulation, the reef top was at a depth of $z_{\mathrm{T}_1} = 5$ m with the right edge of the top at $x_{\mathrm{T}_1} = -10$ m. The top of the reef wall was at $x_{\mathrm{T}_2} = 0.0, z_{\mathrm{T}_2} = 15$ m. The reef slope was the region in between and had a slope of $\psi = 45$ deg. The water IOPs were for Case 1 water with a chlorophyll concentration of 0.5 mg m^{-3}. For a wavelength of 400 nm, for the ray plotted here, this chlorophyll value gives $a = 0.045$ m^{-1}, $b = 0.277$ m^{-1}, and $b_b = 0.0213$. The albedo of single scattering was then $\omega_o = b/(a+b) = 0.860$. Thus at each scattering within the water, the current ray weight w was reduced by a factor of 0.860. The mean free path between scattering events is $1/c = 3.11$ m. The reef top, slope, and wall reflectances were a typical coral reflectance spectrum, which at 400 nm is 0.059. Thus at each reflection of a ray with the coral surface, the ray weight is reduced by a factor of 0.059. A hemispherical scalar irradiance sensor simulating $E_{o\psi}$ was placed on the surface of the reef wall at $[x_{\mathrm{D}}, y_{\mathrm{D}}, z_{\mathrm{D}}]^T = [-5, 0, 10]^T$ m.

The red arrows show a sequence of ray tracks starting at the sensor location. The initial ray was emitted in a direction of about 60 deg relative to the normal to the reef slope. After scattering 11 times within the water (thus reducing the initial weight of $w = 1$ to $0.86^{11} = 0.19$), the ray intersected the reef wall twice (light green rays in the figure) with just one in-water scattering in between. After 13 more in-water scatterings the ray intersected the sea surface (cyan colored rays). This sea-surface-incident ray gives a transmitted ray, which contributes to the estimation of $E_{o\psi}$, and a reflected ray. The sea-surface reflectance (0.025) and transmittance (1 - the reflectance value, so 0.975) were determined by the Fresnel reflection and transmission equations for the angle of incidence of the ray relative to the normal of a randomly generated surface wave facet. The ray incident onto the sea surface had a weight of $w = 8.19 \times 10^{-5}$, so only approximately 0.008% of the sky radiance in the ray-transmitted direction contributes to the estimation of $E_{o\psi}$, for this particular ray. The surface-reflected ray then scattered several more times before its weight dropped below $\epsilon = 10^{-6}$, at which time the ray was killed and a new ray was emitted from the sensor. Figure 5 shows additional views of this same ray sequence. Hundreds of such rays have been examined, and all appear to have the correct behavior.

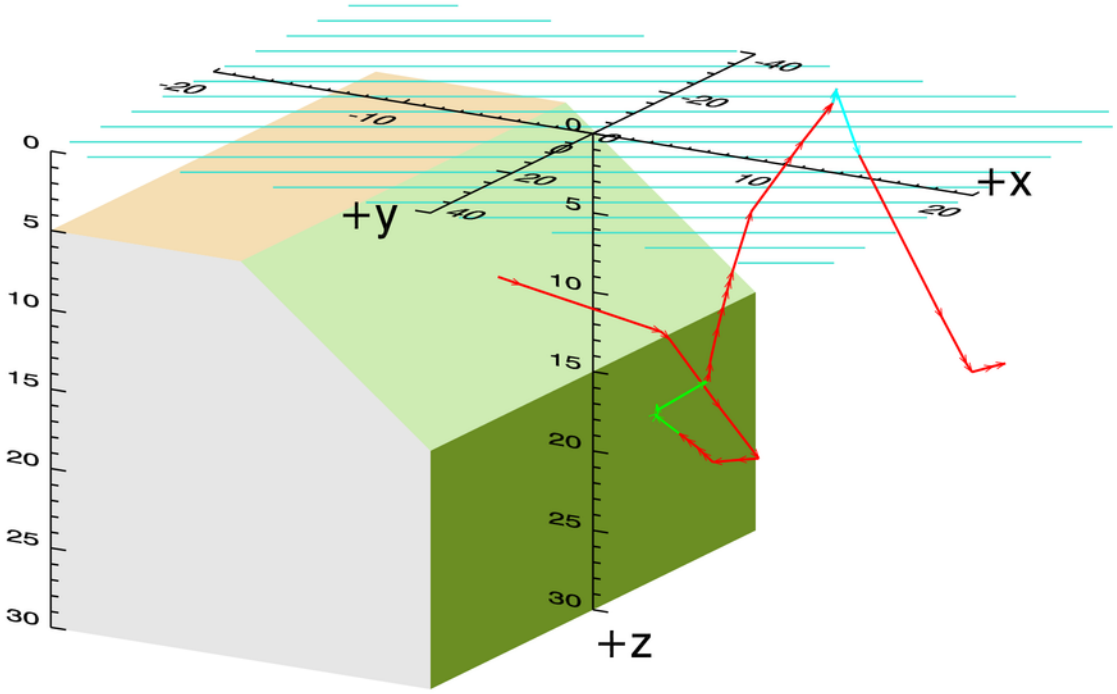

Figure 5: 3D perspective view of example ray tracks resulting from multiple scattering of a single initial ray. The x, y, and z dimensions are not to scale in the plot.

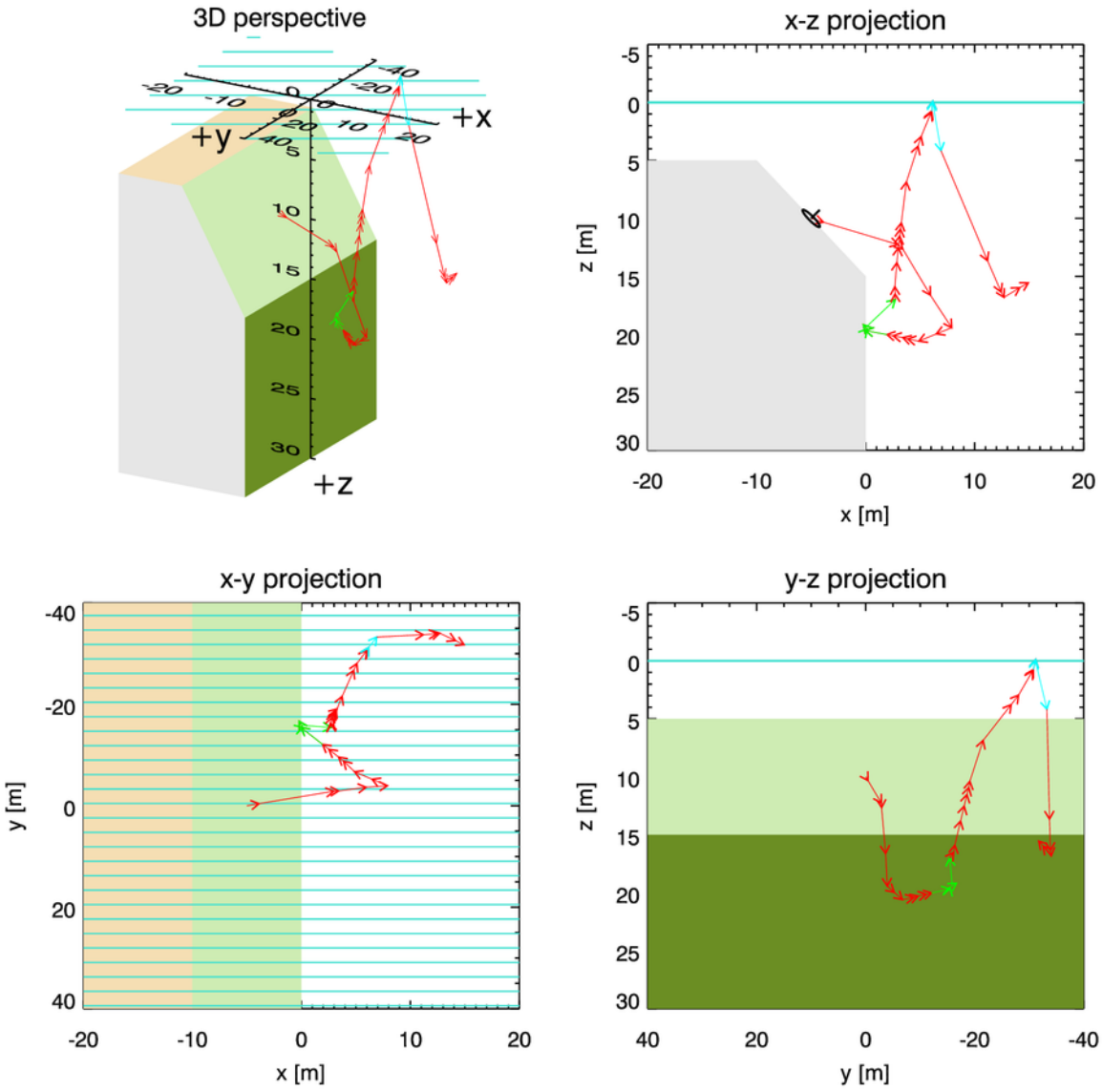

Figure 6: Other views of the ray tracks seen in Fig. 5. The x, y, and z dimensions are not to scale in the plots.

5.3 Comparisons with HydroLight

Quantitative comparisons between the BMC3D code and HydroLight (`www.hydrolight.info` or `http://www.oceanopticsbook.info/view/radiative_transfer_theory/level_2/hydrolight`) can be made for simulations that have a 1D geometry, for which HydroLight can be used. The first of these was for infinitely deep water, and the second was for finite-depth water with a reflecting bottom.

To (approximately) simulate infinitely deep water in the BMC3D code, the reef top was placed at a depth of $z_{\text{top}} = 20$ m and the sensor was placed at an x value of 20 m. Thus the reef should far enough away from the sensor to have a negligible affect on irradiances at depths of 10 m or so. The solar zenith angle was $\theta_{\text{sun}} = 30$ deg and the Radtran sky irradiance model was used for both HydroLight and the BMC3D code. HydroLight 5.3 was run for the same IOP and sky conditions used in the Monte Carlo simulations, but with an infinitely deep bottom boundary condition. The HydroLight-computed radiance distribution $L(z, \theta, \phi)$ was integrated over various hemispheres of direction to obtain irradiances for comparison with the Monte Carlo values. Figure 7 shows the HydroLight-computed depth profiles of E_d, E_u, E_o, and $E_h(\phi_v)$ for azimuthal angles of $\phi_v = 0, 90, 180$ deg. Some difference in the BMC3D and HydroLight values is expected because of statistical noise and numerical algorithms of different types and accuracies. Nevertheless, there is agreement between HydroLight and the BMC3D values within a percent or better, which indicates that the ray tracing is correct, as least as regards in-water and sea-surface interactions. Clearly there are no gross errors (sign errors, missing factors of 2, bad ray tracing logic, etc.) in the BMC3D code, which would lead to large differences between BMC3D and HydroLight.

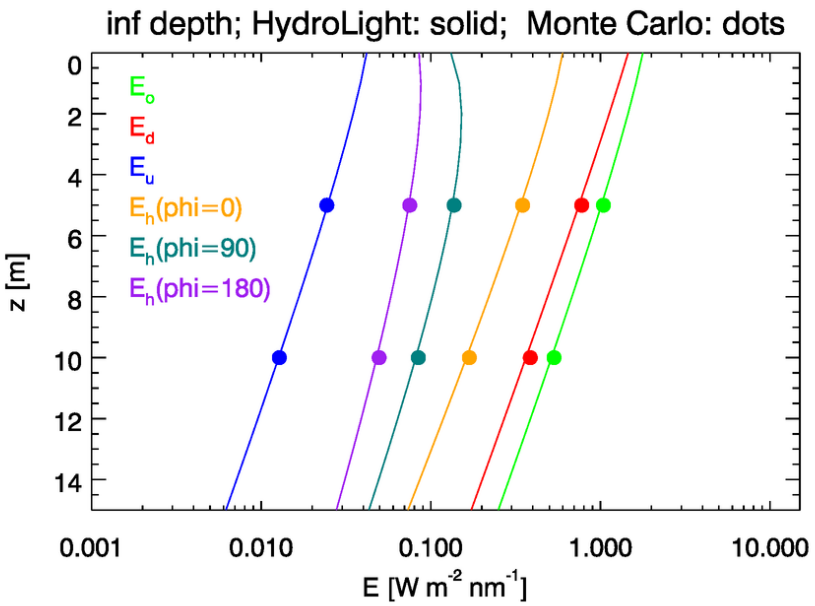

Figure 7: Comparison of HydroLight and BMC3D irradiances for infinitely deep water. Solid lines: irradiances computed by directional integration of the HydroLight-computed radiance distribution. Dots: values computed by BMC3D.

In the BMC3D code for this particular run, any ray that reached a depth of 20 m was killed because it is unlikely than a ray reaching this depth will ever return to the surface, where it can contribute to the desired estimate. Even if a ray does get scattered back to the sea surface, its will have undergone so many scatterings that its weight will make a negligible contribution to the irradiance estimate. The good agreement between the BMC3D and HydroLight values seen in Fig. 7 shows that this approximation does not significantly affect the results. Indeed, further numerical experimentation will likely show that even more rays can be killed without significantly affecting the results.

The BMC3D simulations used 10^8 initial rays to estimate each irradiance. This required about 10 minutes of computer time for each simulation (each point of the figure). (The HydroLight run time was 1 second, which gives all irradiances simultaneously). Even for the estimate of $E_u(z = 10$ m), this resulted in over 2 million rays eventually transmitted through the sea surface, which is enough to make the Monte Carlo statistical noise negligible. In the $E_u(z = 10$ m) simulation, about 0.4% of the energy emitted by the sensor eventually reached the sky. For the $E_d(z = 5$ m) simulation, just over 9% of the emitted energy reached the sky.

For a finite-depth, 1D simulation, the reef top was placed at a depth of $z_{\text{top}} = 5$ m; the reef top reflectance was 0.1. The sensor was placed at $[x_s, y_s, z_s]^T = [-30 \text{ m}, 0, 3 \text{ m}]^T$, which is far enough from the reef top-wall boundary that the end of the reef top will not be seen by most rays. This geometry gives many reflections of rays back and forth between the sea surface and the reef top, and thus tests the correctness of the treatment of the reef top BRDF calculations. The BMC3D simulations used 10^6 initial rays to estimate each irradiance. HydroLight was run for a reflecting bottom at 5 m depth. Figure 8 shows the excellent agreement between the BMC3D code and HydroLight.

Figures 7 and 8 show results for a solar zenith angle of $\theta_{\text{sun}} = 30$ deg and a wavelength of 475 nm. As mentioned in the abstract, one run of the code actually generates results for a range of solar zenith and azimuthal angles. Such output is shown in Fig. 9. The orange, green, and purple curves show values of $E_h(\phi_v = 0, z = 5$ m) for solar zenith angles of $\theta_{\text{sun}} = 0$, 10, ..., 80 deg, and solar azimuthal angles of $\phi_{\text{sun}} = 0$, 90, and 180 deg. The dots on these curves at $\theta_{\text{sun}} = 30$ correspond to the dots of the same color at 5 m depth in Fig. 7. The red curve shows the total sun and sky irradiance incident onto the sea surface at 475 nm; the red dots show the 10 deg angular resolution used in the runs. The blue curve shows the HydroLight-computed values of $E_d(z = 5$ m). The difference in the $E_d(z = 5$ m) curve and the three $E_h(\phi_v = 0, z = 5$ m) curves illustrates the large differences in downwelling and horizontally viewed plane irradiances.

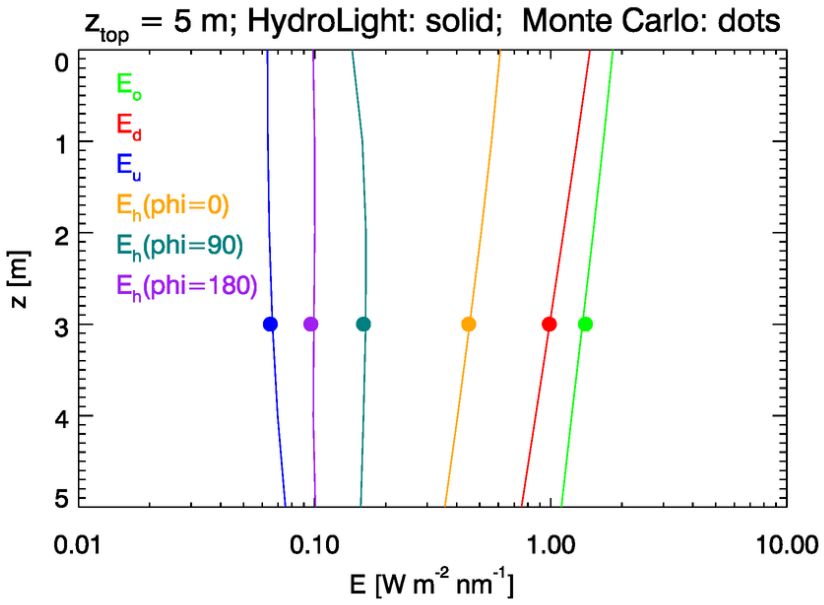

Figure 8: Comparison of HydroLight and BMC3D irradiances for 5 m deep water. Solid lines: irradiances computed by directional integration of the HydroLight-computed radiance distribution. Dots: values computed by BMC3D.

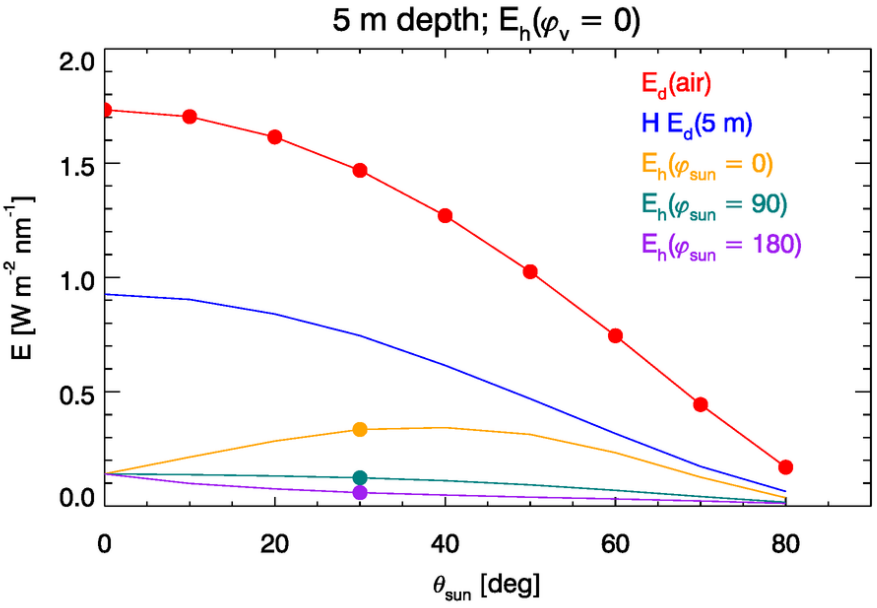

Figure 9: Example output from one run, for which the same ray tracing yields estimates for a range of sun and sky conditions.

A In-water Ray Scattering

The generation of new rays by in-water scattering is central to the ray-tracing process, and these calculations are somewhat complicated. It is therefore worthwhile to review in detail how ray scattering is effected in Monte Carlo codes. Although the coordinate system transformations developed in this Appendix are standard (e.g., Bower, 2012 or Cheston, 1966), the needed equations are included in this document for completeness and for convenient referencing in the BMC3D source code.

Recalling Eq. (3), let $\mathbf{R}'$ denote an initial ray with starting point $\mathbf{r}_1$ and ending point $\mathbf{r}_2$. This ray is traveling in direction (θ, ϕ) in the ocean coordinate system, as seen in Fig. 10. An in-water ray can be anywhere in the water and traveling in any direction, so the local coordinate systems used for the coral reef surfaces are not applicable to the calculation of scattered rays. It is therefore necessary to define a local (at the point of scattering) coordinate system for scattering calculations. The scattering angles γ and α will then be applied in this system to determine the direction of the scattered ray $\mathbf{R}$. (The use of primes, e.g. $\mathbf{R}'$, for initial or unscattered rays and unprimed variables, e.g. $\mathbf{R}$, for scattered rays conforms to the convention used in *Light and Water* and is used in the BMC3D source code.)

In the ocean system, ray $\mathbf{R}'$ has components (R'_x, R'_y, R'_z):

$$\begin{aligned}\mathbf{R}' &= R'_x\,\hat{\mathbf{x}} + R'_y\,\hat{\mathbf{y}} + R'_z\,\hat{\mathbf{z}} \\ &= R'\sin\theta\cos\phi\,\hat{\mathbf{x}} + R'\sin\theta\sin\phi\,\hat{\mathbf{y}} + R'\cos\theta\,\hat{\mathbf{x}}\,,\end{aligned} \tag{41}$$

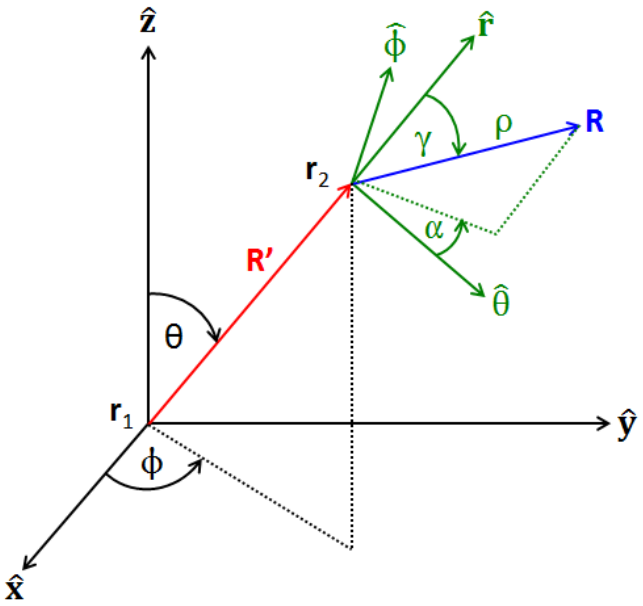

Figure 10: Coordinate systems used to describe the scattering of an in-water ray. The initial or unscattered ray $\mathbf{R}'$ is shown in red; the scattered ray $\mathbf{R}$ is blue. The ocean coordinate system and angles measured in this system are in black, and the local coordinate system and angles measured in the local system are green.

where the cartesian components R'_x etc., in terms of spherical coordinates come from inspection of Fig. 10. R' is the length of the vector $\mathbf{R}'$.

A convenient local coordinate system $(\hat{\mathbf{r}}, \hat{\theta}, \hat{\phi})$ for scattered rays is constructed as follows. The radial unit vector

$$\hat{\mathbf{r}} = \frac{\mathbf{R}'}{R'} = \frac{\mathbf{r}_2 - \mathbf{r}_1}{|\mathbf{r}_2 - \mathbf{r}_1|}$$

is in the same direction as the initial ray. The azimuthal unit vector $\hat{\phi}$ is defined by the cross product of the ocean coordiante system $\hat{\mathbf{z}}$ and the incident vector's direction:

$$\hat{\phi} = \frac{\hat{\mathbf{z}} \times \hat{\mathbf{r}}}{|\hat{\mathbf{z}} \times \hat{\mathbf{r}}|} \,.$$

This vector points in the direction of increasing ϕ values. (If the unscattered vector is in the same direction as $\hat{\mathbf{z}}$, the direction of $\hat{\phi}$ can be chosen at random.) The polar unit vector is then given by

$$\hat{\theta} = \hat{\phi} \times \hat{\mathbf{r}} \,.$$

This vector points in the direction of increasing θ values. The $(\hat{\mathbf{r}}, \hat{\theta}, \hat{\phi})$ system is then an orthogonal system of coordinates in which the scattering angles can be applied to define the direction of the scattered ray. However, these directions are not fixed in the ocean system; they depend on the direction of the unscattered ray.

To express the local coordinate system directions in the ocean system, note that the radial unit vector $\hat{\mathbf{r}}$ can be thought of as the normalized rate of change $\mathbf{R}'$ with respect to length R':

$$\hat{\mathbf{r}} = \frac{1}{\left|\frac{\partial \mathbf{R}'}{\partial R'}\right|} \frac{\partial \mathbf{R}'}{\partial R'} \,.$$

Equation (41) then gives

$$\hat{\mathbf{r}} = \sin\theta\cos\phi\,\hat{\mathbf{x}} + \sin\theta\sin\phi\,\hat{\mathbf{y}} + \cos\theta\,\hat{\mathbf{z}} \,, \tag{42}$$

after noting that $|\partial \mathbf{R}'/\partial R'| = 1$. In the same fashion, $\hat{\theta}$ and $\hat{\phi}$ can be written as

$$\hat{\theta} = \frac{1}{\left|\frac{\partial \mathbf{R}'}{\partial \theta}\right|} \frac{\partial \mathbf{R}'}{\partial \theta} \qquad \text{and} \qquad \hat{\phi} = \frac{1}{\left|\frac{\partial \mathbf{R}'}{\partial \phi}\right|} \frac{\partial \mathbf{R}'}{\partial \phi} \,.$$

After noting that $|\partial \mathbf{R}'/\partial\theta| = R'$ and $|\partial \mathbf{R}'/\partial\phi| = R'\sin\theta$, the same process gives

$$\begin{aligned} \hat{\theta} &= \cos\theta\cos\phi\,\hat{\mathbf{x}} + \cos\theta\sin\phi\,\hat{\mathbf{y}} - \sin\theta\,\hat{\mathbf{z}} \\ \hat{\phi} &= -\sin\theta\,\hat{\mathbf{x}} + \cos\theta\,\hat{\mathbf{y}} \,. \end{aligned}$$

Now consider an arbitrary vector point function $\mathbf{G}(\mathbf{R}')$. ($\mathbf{G}(\mathbf{R}')$ might be, for example, the value of an electric field at spatial point $\mathbf{R}'$.) In the cartesian ocean system, $\mathbf{G}(\mathbf{R}')$ is written in component form as

$$\mathbf{G}(\mathbf{R}') = G'_x\,\hat{\mathbf{x}} + G'_y\,\hat{\mathbf{y}} + G'_z\,\hat{\mathbf{z}} \,.$$

In the local system, $\mathbf{G}(\mathbf{R}')$ is written as

$$\mathbf{G}(\mathbf{R}') = G'_r\,\hat{\mathbf{r}} + G'_\theta\,\hat{\theta} + G'_\phi\,\hat{\phi} \,.$$

The relations between the components of $\mathbf{G}(\mathbf{R}')$ in these two coordinate systems are obtained as follows. The radial component of $\mathbf{G}(\mathbf{R}')$ is

$$G'_r = \mathbf{G}(\mathbf{R}') \cdot \hat{\mathbf{r}} = G'_x(\hat{\mathbf{x}} \cdot \hat{\mathbf{r}}) + G'_y(\hat{\mathbf{y}} \cdot \hat{\mathbf{r}}) + G'_z(\hat{\mathbf{z}} \cdot \hat{\mathbf{r}}) \,.$$

However, from Eq. (42)

$$\begin{bmatrix} \hat{\mathbf{x}} \cdot \hat{\mathbf{r}} \\ \hat{\mathbf{y}} \cdot \hat{\mathbf{r}} \\ \hat{\mathbf{z}} \cdot \hat{\mathbf{r}} \end{bmatrix} = \begin{bmatrix} \sin\theta\cos\phi \\ \sin\theta\sin\phi \\ \cos\theta \end{bmatrix} ,$$

so that

$$G'_r = G'_x \sin\theta\cos\phi + G'_y \sin\theta\sin\phi + G'_z \cos\theta \,.$$

In the same fashion we find

$$\begin{aligned} G'_\theta &= G'_x \cos\theta\cos\phi + G'_y \cos\theta\sin\phi - G'_z \sin\theta \\ G'_\phi &= -G'_x \sin\phi + G'_y \cos\phi \,. \end{aligned}$$

Writing these results in matrix form gives

$$\begin{bmatrix} G'_r \\ G'_\theta \\ G'_\phi \end{bmatrix} = \begin{bmatrix} \sin\theta\cos\phi & \sin\theta\sin\phi & \cos\theta \\ \cos\theta\cos\phi & \cos\theta\sin\phi & -\sin\theta \\ -\sin\phi & \cos\phi & 0 \end{bmatrix} \begin{bmatrix} G'_x \\ G'_y \\ G'_z \end{bmatrix} .$$

The inverse gives (G'_x, G'_y, G'_z) in terms of $(G'_r, G'_\theta, G'_\phi)$:

$$\begin{bmatrix} G'_x \\ G'_y \\ G'_z \end{bmatrix} = \begin{bmatrix} \sin\theta\cos\phi & \cos\theta\cos\phi & -\sin\phi \\ \sin\theta\sin\phi & \cos\theta\sin\phi & \cos\phi \\ \cos\theta & -\sin\theta & 0 \end{bmatrix} \begin{bmatrix} G'_r \\ G'_\theta \\ G'_\phi \end{bmatrix} . \tag{43}$$

Now let the vector point function $\mathbf{G}(\mathbf{R}')$ be the end point of the scattered vector $\mathbf{R}$ at location $\mathbf{R}'$. (In the electric field analogy, $\mathbf{R}$ is the electric field at $\mathbf{G}(\mathbf{R}')$. The field has magnitude ρ and direction (γ, α) in the local system.) Inspection of Fig. 10 shows that

$$\mathbf{G}(\mathbf{R}') = \begin{bmatrix} G'_r \\ G'_\theta \\ G'_\phi \end{bmatrix} = \mathbf{R} = \begin{bmatrix} \rho\cos\gamma \\ \rho\sin\gamma\cos\alpha \\ \rho\sin\gamma\sin\alpha \end{bmatrix} .$$

Inserting these values into Eq. (43) and remembering that the origin of the $(\hat{\mathbf{r}}, \hat{\theta}, \hat{\phi})$ system is at point $\mathbf{r}_2$ gives

$$\begin{bmatrix} x \\ y \\ z \end{bmatrix} = \begin{bmatrix} x_2 \\ y_2 \\ z_2 \end{bmatrix} + \begin{bmatrix} \sin\theta\cos\phi & \cos\theta\cos\phi & -\sin\phi \\ \sin\theta\sin\phi & \cos\theta\sin\phi & \cos\phi \\ \cos\theta & -\sin\theta & 0 \end{bmatrix} \begin{bmatrix} \rho\cos\gamma \\ \rho\sin\gamma\cos\alpha \\ \rho\sin\gamma\sin\alpha \end{bmatrix} . \tag{44}$$

This equation gives the location of the end point of the scattered ray $\mathbf{R}$ in the ocean coordinate system. To continue tracing the scattered ray, the unscattered point $\mathbf{r}_2$ becomes the new $\mathbf{r}_1$, and the scattered ray endpoint at $\mathbf{R} = [x, y, z]^{\mathrm{T}}$ becomes the new $\mathbf{r}_2$.

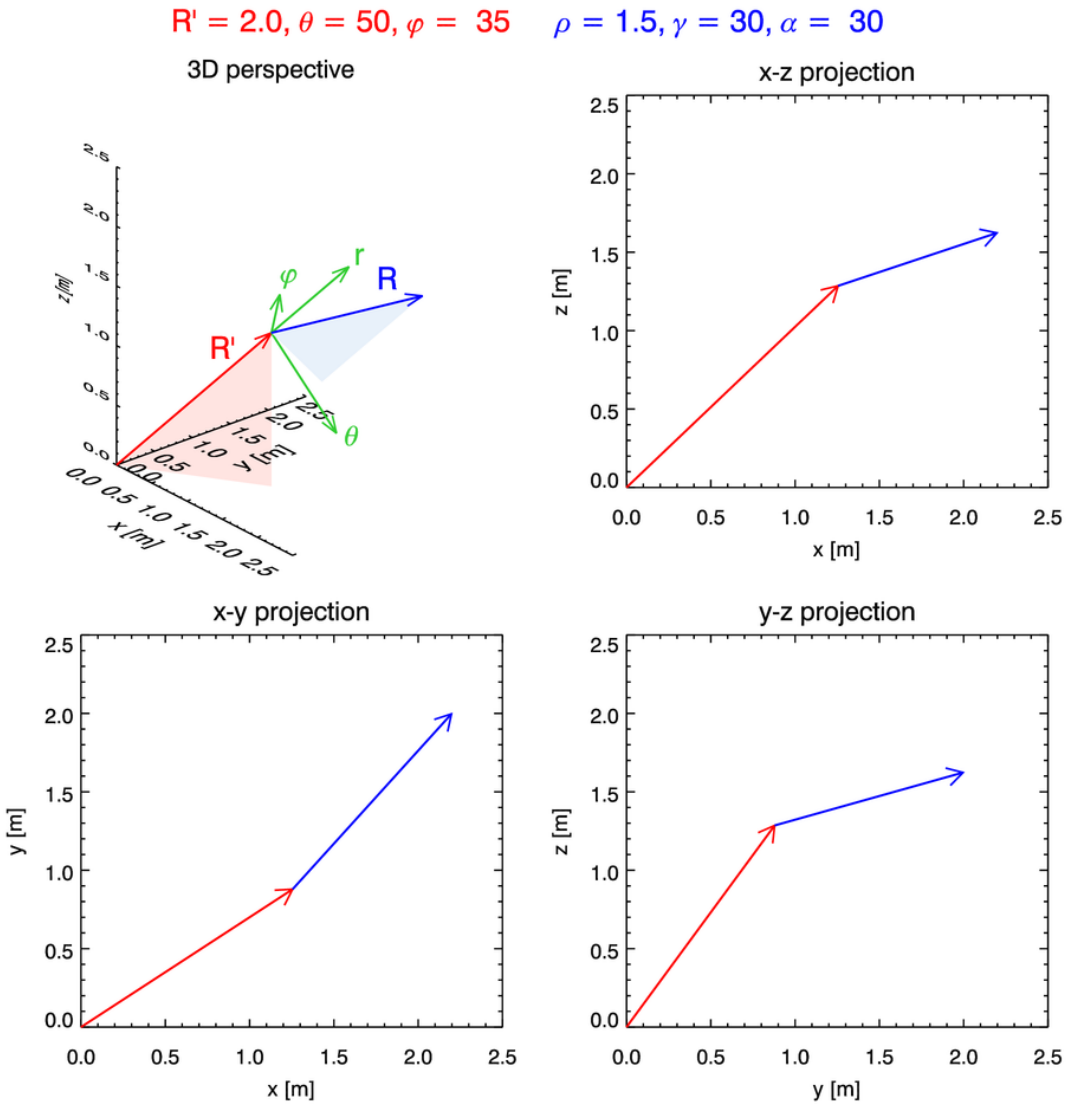

Figure 11: Example of unscattered (red arrows) and scattered (blue arrows) rays for the (R', θ, ϕ) and (ρ, γ, α) values shown at the top. As in Fig. 10, in the upper left panel, the black axes are the fixed ocean coordinate system, and the green axes are the local system for the scattered ray. The rose and light blue triangles show the azimuthal planes of the red and blue vectors, respectively. The other panels shows projections of the rays onto the planes of the ocean coordinate system, which allows easy checking the numerical values in the output.

To aid in debugging the BMC3D code, an IDL plot program was written to show graphically the unscattered and scattered rays for any values of (R', θ, ϕ) and (ρ, γ, α). Figure 11 shows an example output. The panels of these figures, along with the digital output (not shown), give both visual and quantitative checks on the correctness Eq. (44) and the associated quantities.

In BMC3D, ρ is determined by Eq. (26), γ is determined according to the scattering phase function used in the simulation, and α is randomly chosen to be azimuthally isotropic. Equation (44) is then used to obtain the end point of the scattered ray in the ocean system.

How γ is determined for an arbitrary scattering phase function $\tilde{\beta}(\gamma)$ is described in detail at `http://www.oceanopticsbook.info/view/monte_carlo_simulation/introduction`. For azimuthally isotropic scattering, the end result is that the scattering angle γ is determined by solving the equation

$$\mathfrak{R} = 2\pi \int_0^{\gamma} \tilde{\beta}(\gamma') \, \sin\gamma' \, d\gamma' \,, \tag{45}$$

where $\mathfrak{R}$ is a uniform (0,1) random number. In general this solution must be obtained numerically. In practice, this can be done most efficiently by first building a look-up table of values of the integral of Eq. (45) for closely space values of γ from 0 to π. This look-up table is then the cumulative distribution function for the phase function, which is viewed as a probability distribution function for the scattering angle γ. The random number $\mathfrak{R}$ can then be used in this look-up table to obtain the value of γ.

B Ray Initialization

When a ray is initialized from a detector, values of polar and azimuthal angles (γ, α) are randomly determined according to the detector's angular response. These values of (γ, α) are in a local coordinate system for the detector. This system will be one of the reef local systems if the detector is on the surface of the coral, but if the detector is within the water water, this will be a system defined by the detector's orientation $(\theta_{\mathrm{D}}, \phi_{\mathrm{D}})$ in the ocean system. In either case, the initial ray can be treated just as if it were a scattered ray created by a scattering event at the location of the detector. The initial ray's ρ value is determined using Eq. (26), and the initial weight is $w = 1$. The initial ray endpoint is then converted into ocean coordinates using transformation (44), just as for scattered rays.

A plane irradiance sensor (cosine detector) has a detecting *surface material* that is equally sensitive to radiance from any direction; the cosine response comes from the change in the apparent detector surface area for off-axis viewing directions. The detector material is assumed to be azimuthally isotropic. Let the polar (off-axis) angular response of the detector material be $\sigma(\gamma)$. Then the material of a cosine detector has $\sigma(\gamma) = \sigma_o$, independent of γ, which gives a cosine response of the detector as a whole, including the geometric effect of the apparent detector surface area for different viewing directions. In backward Monte Carlo ray tracing, rays are emitted from the detector location in an angular pattern that mimics the response of the detector to incoming rays.

In general for an azimuthally isotropic sensor whose polar (off-axis) angular response is $\sigma(\gamma')$,

the random value of γ is determined by solving (Modest, 1993, Eq. 19.32.)

$$\mathfrak{R} = \frac{\int_0^{\gamma} \sigma(\gamma') \cos\gamma' \, \sin\gamma' \, d\gamma'}{\int_0^{\pi/2} \sigma(\gamma') \cos\gamma' \, \sin\gamma' \, d\gamma'} \,, \tag{46}$$

where $\mathfrak{R}$ is a uniform (0,1) random number. (See `http://www.oceanopticsbook.info/view/monte_carlo_simulation/level_2/the_brdf_as_a_pdf` for further discussion of how a cosine-reflecting material leads to a surface whose reflected *radiance* is independent of viewing direction.)

In this case of a cosine collector or emitter, Eq. (46) yields

$$\mathfrak{R} = \sin^2\gamma \,,$$

or

$$\gamma = \sin^{-1}(\sqrt{\mathfrak{R}}) \,. \tag{47}$$

This peculiar looking formula for γ is precisely what is needed to make the angular distribution of rays emitted from a detector in a backward Monte Carlo simulation mimic the cosine response of a plane irradiance sensor. (Since $\int_0^{\gamma} \cos\gamma' \sin\gamma' d\gamma'$ can be written either as $\frac{1}{2}\sin^2\gamma$ or as $\frac{1}{2}(1-\cos^2\gamma)$, the equation for γ can also be written as $\gamma = \cos^{-1}(\sqrt{\mathfrak{R}})$ after noting that $1-\mathfrak{R}$ has the same statistical distribution as $\mathfrak{R}$. Ray by ray the γ values will be different for the same value of $\mathfrak{R}$, but the statistical distribution of γ values resulting from a large number of emitted rays will be the same, which is what matters in Monte Carlo simlations.)

Consider a "top-hat" detector whose collecting surface is equally sensitive to radiance over $0 \le \gamma \le \gamma_{\mathrm{D}}$ and zero for $\gamma > \gamma_{\mathrm{D}}$; that is, $\sigma(\gamma')$ is constant from 0 to γ_{D} and 0 for $\gamma > \gamma_{\mathrm{D}}$. Equation (46) then yields

$$\gamma = \sin^{-1}(\sin\gamma_{\mathrm{D}}\sqrt{\mathfrak{R}}) \,. \tag{48}$$

This distribution of emission angles is used to simulate a radiance detector with a viewing direction half-angle of γ_{D}.

Another way to view emission from the detector is to think of the emitted ray as a ray that has been created by scattering at the location of the point detector. For example, one can imagine a ray incident onto the surface from "behind" or "within" the surface, and then being scattered (emitted) outward from the surface into the water. For a phase function that scatters (emits) in a cosine pattern, the scattering phase function is

$$\tilde{\beta}(\gamma) = \begin{cases} \frac{1}{\pi}\cos\gamma & \text{if } 0 \le \gamma \le \pi/2 \\ 0 & \text{if } \pi/2 < \gamma \le \pi \,. \end{cases}$$

Inserting this phase function into Eq. (45) leads again to $\gamma = \sin^{-1}(\sqrt{\mathfrak{R}})$.

The viewpoint of emission as a scattering process readily yields the formulas needed for emission by scalar irradiance detectors. For a hemispherical scalar irradiance detector, corresponding to isotropic emission into $0 \le \gamma \le \pi/2$, the equivalent scattering phase function is

$$\tilde{\beta}(\gamma) = \begin{cases} \frac{1}{2\pi} & \text{if } 0 \le \gamma \le \pi/2 \\ 0 & \text{if } \pi/2 < \gamma \le \pi \,. \end{cases}$$

Inserting this phase function into Eq.(45) gives

$$\gamma = \cos^{-1}(1 - \mathfrak{R})\,. \tag{49}$$

Note that this γ can range from 0 to 90 deg. For a scalar irradiance detector, the equivalent phase function is $\tilde{\beta}(\gamma) = 1/(4\pi), 0 \le \gamma \le \pi$, and the resulting equation for the emission angle is

$$\gamma = \cos^{-1}(1 - 2\mathfrak{R})\,, \tag{50}$$

which gives γ values between 0 and 180 deg.

In all cases, the azimuthal angle is determined from

$$\alpha = 2\pi\mathfrak{R}\,. \tag{51}$$

C Reflection and Transmission of Rays at a Wind-blown Sea Surface

As previously mentioned, if a ray crosses the mean sea surface at $z = 0$, it is reflected and transmitted by the wind-blown sea surface. These calculations proceed as follows.

First, a unit vector normal to the sea surface is randomly generated in accordance with the Cox-Munk wind speed-wave slope law for the wind speed U of the simulation. Let $\eta(x, y)$ be the elevation of the wind-blown sea surface, and let the wind be blowing in the $+\hat{\mathbf{x}}$ direction. Then the along-wind and cross-wind slopes of the sea surface are

$$\eta_{\mathrm{a}} = \frac{\partial \eta}{\partial x} \qquad \text{and} \qquad \eta_{\mathrm{c}} = \frac{\partial \eta}{\partial \mathrm{y}}\,. \tag{52}$$

Is is known from experiment (Cox and Munk, 1954; *Light and Water* page 168) that the slopes η_{a} and η_{c} are gaussianly distributed about a zero mean with variances

$$\sigma_{\mathrm{a}}^2 = 3.16 \cdot 10^{-3} U \qquad \text{and} \qquad \sigma_{\mathrm{c}}^2 = 1.92 \cdot 10^{-3}\mathrm{U}\,, \tag{53}$$

where U is in meters per second at 12.5 m above mean sea level. Let $\mathfrak{R}$ be a random number drawn from a gaussian distribution with zero mean and unit variance, denoted by $\mathfrak{R} \sim \mathfrak{G}(0, 1)$. Then if $\mathfrak{R}_1$ and $\mathfrak{R}_2$ are independently drawn random numbers from $\mathfrak{G}(0, 1)$,

$$\eta_{\mathrm{a}} = \mathfrak{G}_1\, \sigma_{\mathrm{a}} \qquad \text{and} \qquad \eta_{\mathrm{c}} = \mathfrak{G}_2\, \sigma_{\mathrm{c}} \tag{54}$$

have the required variances for sea surface slopes. The associated outward (facing the sky) normal to the sea surface is then

$$\hat{\mathbf{n}} = \frac{\eta_{\mathrm{a}}\hat{\mathbf{x}} + \eta_{\mathrm{c}}\hat{\mathbf{y}} - \hat{\mathbf{z}}}{[\eta_{\mathrm{a}}^2 + \eta_{\mathrm{c}}^2 + 1]^{1/2}}\,. \tag{55}$$

Note that $\hat{\mathbf{n}} = -\hat{\mathbf{z}}$ if the sea surface is level.

Let $\hat{\xi}', \hat{\xi}_{\mathrm{r}}$ and $\hat{\xi}_{\mathrm{t}}$ be unit vectors in the directions of the incident, reflected, and transmitted rays, respectively. (As before, a primed variable indicates the incident ray, and unprimed variables indicate scattered (reflected or transmitted) rays.) The incident ray that reaches the sea surface is

traveling in direction (θ, ϕ) in the ocean coordinate system. This direction is described by a unit vector

$$\begin{aligned}\hat{\xi}' &= \xi'_x\,\hat{\mathbf{x}} + \xi'_y\,\hat{\mathbf{y}} + \xi'_z\,\hat{\mathbf{z}} \\ &= \sin\theta\cos\phi\,\hat{\mathbf{x}} + \sin\theta\sin\phi\,\hat{\mathbf{y}} + \cos\theta\,\hat{\mathbf{z}}\,. \end{aligned} \tag{56}$$

The dot product between $\hat{\mathbf{n}}$ and $\hat{\xi}'$ gives the angle of incidence θ' of the ray onto the sloping sea surface:

$$\theta' = \cos^{-1}(\hat{\xi}' \cdot \hat{\mathbf{n}})\,. \tag{57}$$

This is the angle relative to the normal to the surface at the point where the incident ray is reflected back into the water by the underside of the sea surface. There is also usually a transmitted ray whose direction relative to the surface normal is given by Snel's law (and, yes, the guy's name was Snel not Snell)

$$\theta_{\rm t} = \sin^{-1}\left(n_{\rm w}\sin\theta'\right)\,, \tag{58}$$

where $n_{\rm w}$ is the real index of refraction of the water. If the argument of the inverse sine is greater than 1, then there is total internal reflection and no ray is transmitted into the air.

The incident and transmitted angles θ' and $\theta_{\rm t}$ are then used in Fresnel's formula for the reflectance of the sea surface,

$$R_{\rm F}(\theta') = \frac{1}{2}\left(\left[\frac{\sin(\theta'-\theta_{\rm t})}{\sin(\theta'+\theta_{\rm t})}\right]^2 + \left[\frac{\tan(\theta'-\theta_{\rm t})}{\tan(\theta'+\theta_{\rm t})}\right]^2\right)\,, \tag{59}$$

which holds for $\theta' \neq 0$. If $\theta' = 0$, the Fresnel reflectance is given by

$$R_{\rm F}(\theta'=0) = \left(\frac{n_{\rm w}-1}{n_{\rm w}+1}\right)^2\,.$$

The weight w of the incident ray is multiplied by $R_{\rm F}$ to get the weight of the reflected ray. The weight of the transmitted ray is then $(1-R_{\rm F})w$. The weights of the reflected plus transmitted rays thus equal the weight of the incident ray; in other words, energy is conserved at the sea surface.

The directions of $\hat{\xi}_{\rm r}$ and $\hat{\xi}_{\rm t}$ relative to the tilted wave facet are (*Light and Water* Eq. 4.12)

$$\hat{\xi}_{\rm r} = \hat{\xi}' - 2(\hat{\xi}'\cdot\hat{\mathbf{n}})\,\hat{\mathbf{n}} \tag{60}$$

$$\hat{\xi}_{\rm t} = n_{\rm w}\hat{\xi}' - c\hat{\mathbf{n}}\,, \tag{61}$$

where

$$c = n_{\rm w}\hat{\xi}'\cdot\hat{\mathbf{n}} - \left[(n_{\rm w}\hat{\xi}'\cdot\hat{\mathbf{n}})^2 - n_{\rm w}^2 + 1\right]^{1/2}\,.$$

Note that both of these vectors lie in the plane determined by $\hat{\xi}'$ and $\hat{\mathbf{n}}$.)

Both $\hat{\xi}'$ and $\hat{\mathbf{n}}$ are specified in the ocean coordinate system. Therefore the equations for $\hat{\xi}_{\rm r}$ and $\hat{\xi}_{\rm t}$ give values that are also in the ocean coordinate system. Thus these vectors do not need to be transformed into the ocean system, as must be done for in-water scattered rays.

If the surface is not level (i.e., the wind speed U is not zero), it can happen that the surface is tilted so much that a near-grazing incident ray is reflected into a slightly upward direction, or that a transmitted ray is traveling in a slightly downward direction. In a real ocean, these rays

would encounter the sea surface again at a nearby point and be reflected and transmitted again. In the BMC3D code, such rays are flagged as anomolous and are dropped. Simulation results show that there are only a few anomolous rays out of every 1000 rays incident onto the sea surface, so dropping these rays has a negligible effect on the computed radiometric values.

As with the in-water scattering calculations, an IDL plot routine was written to check the preceding equations. Figure 12 shows an example plot generated by this routine. In this example, the surface along-wind and cross-wind slopes were $\eta_a = 0.2$ and $\eta_c = 0.15$, which correspond to slope angles of $\theta_a = 11.3$ and $\theta_c = 8.5$ degrees. A positive η_a (η_c) means that the surface slopes downward in the $+\hat{\mathbf{x}}$ ($+\hat{\mathbf{y}}$) direction. The green triangle in the figure shows a facet of the sea surface with these slopes. The outward normal $\hat{\mathbf{n}}$ tilts towards the $+\hat{\mathbf{x}}$, $+\hat{\mathbf{y}}$ quadrant by 11.8 deg from the $-\hat{\mathbf{z}}$ axis.

An incident ray $\hat{\xi}'$ traveling in the $\theta = 150, \phi = 0$ direction is incident onto the underside of the sea surface. (Remember that θ is measured from the $+\hat{\mathbf{z}}$ direction, so an upward-traveling ray has $\theta > 90$ deg.) This ray has angles of incidence $\theta' = 18.96$ and transmission $\theta_t = 25.81$ deg., relative to the normal to the tilted sea surface. These are the angles used in Eq. (59). The polar and azimuthal angles of $\hat{\xi}_\mathrm{t}$ in the ocean system are 143.2 and -5.16 deg., respectively. These are the angles used to tally the transmitted ray to the appropriate sky angular bin. It is not obvious from the perspective of this plot, but the digital output (or a different rotation of the plot axes) shows that $\hat{\mathbf{n}}, \hat{\xi}', \hat{\xi}_\mathrm{r}$ and $\hat{\xi}_\mathrm{t}$ are co-planar, as expected.

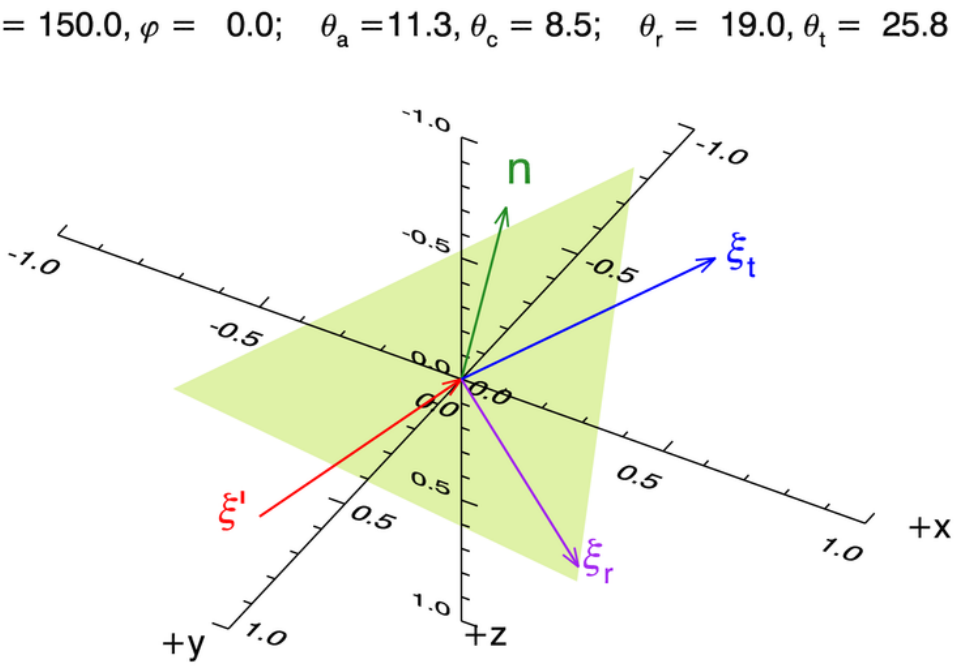

Figure 12: An example ray plot as used for debugging the code for ray-sea surface interactions. The green triangle is a tilted wave facet on the sea surface; the outward normal to this surface is $\hat{\mathbf{n}}$. The red arrow is an upward traveling incident ray $\hat{\xi}'$. The reflected ray $\hat{\xi}_\mathrm{r}$ is purple, and the transmitted ray $\hat{\xi}_\mathrm{t}$ is blue.

6 References

Bower, A. F., 2012. *Applied Mechanics of Solids.* Online text at `www.solidmechanics.org`.

Cheston, W. B., 1964. *Elementary Theory of Electric and Magnetic Fields.* John Wyley and Sons, New York, 319 pages.

Cox, C. and W. Munk, 1954. Statistics of the sea surface derived from sun glitter. *J. Marine Res.* 13, 198-227.

Gordon, H. R., 1985. Ship perturbation of irradiance measurements at sea. 1: Monte Carlo simulations. *Appl. Optics* 24(23), 4172-4182.

Lesser, M. P, M. Slattery, and C. D. Mobley, 2018. Biodiversity and functional ecology of mesophotic coral reefs. *Annual Review of Ecology, Evolution, and Systematics.* (in press)

Light and Water: Mobley, C. D., 1994. *Light and Water: Radiative Transfer in Natural Waters.* Academic Press, 592 pages. Available online at `http://www.oceanopticsbook.info/view/introduction/level_2/text_books_relevant_to_ocean_optics`.

Mobley, C. D. and L. K. Sundman, 2003. Effects of optically shallow bottoms on upwelling radiances: Inhomogeneous and sloping bottoms. *Limnol. Oceanogr.* 48(1, part 2), 329-336.

Modest, M. F., 1993. *Radiative Heat Transfer.* McGraw-Hill, 832 pages.